# *Bifurcation analysis of a diffusive ratio-dependent predator–prey model*

**Yongli Song & Xingfu Zou**

**Nonlinear Dynamics**
An International Journal of Nonlinear Dynamics and Chaos in Engineering Systems

ISSN 0924-090X
Volume 78
Number 1

Nonlinear Dyn (2014) 78:49-70
DOI 10.1007/s11071-014-1421-2

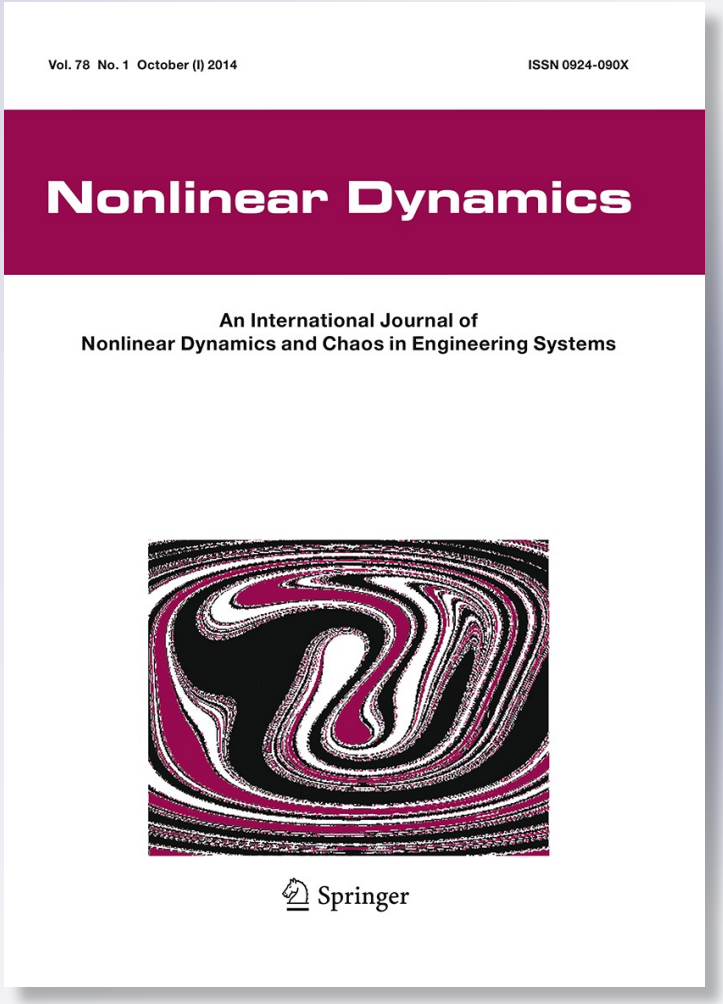


Springer

Nonlinear Dyn (2014) 78:49–70
DOI 10.1007/s11071-014-1421-2

ORIGINAL PAPER

# Bifurcation analysis of a diffusive ratio-dependent predator–prey model

**Yongli Song · Xingfu Zou**

Received: 24 January 2014 / Accepted: 11 April 2014 / Published online: 7 May 2014


**Abstract** In this paper, a ratio-dependent predator–prey model with diffusion is considered. The stability of the positive constant equilibrium, Turing instability, and the existence of Hopf and steady state bifurcations are studied. Necessary and sufficient conditions for the stability of the positive constant equilibrium are explicitly obtained. Spatially heterogeneous steady states with different spatial patterns are determined. By calculating the normal form on the center manifold, the formulas determining the direction and the stability of Hopf bifurcations are explicitly derived. For the steady state bifurcation, the normal form shows the possibility of pitchfork bifurcation and can be used to determine the stability of spatially inhomogeneous steady states. Some numerical simulations are carried out to illustrate and expand our theoretical results, in which, both spatially homogeneous and heterogeneous periodic solutions are observed. The numerical simulations also show the coexistence of two spatially inhomogeneous steady states, confirming the theoretical prediction.

Y. Song
Department of Mathematics, Tongji University,
Shanghai 200092, People's Republic of China

X. Zou (✉)
Department of Applied Mathematics,
University of Western Ontario,
London, Ontario N6A 5B7, Canada
e-mail: xzou@uwo.ca

**Keywords** Predator–prey · Diffusion · Ratio dependent · Turing instability · Hopf bifurcation · Pitchfork bifurcation · Normal form

## 1 Introduction

Predator–prey interactions in nature are largely responsible for the rich biodiversity of complex ecosystems [3]. As such, qualitative and quantitative analysis on the predator–prey relationships is of practical and theoretical significance and has been an important area in population biology. A classical predator–prey model without considering the spatial effect is the following system of ordinary differential equations:

$$\begin{cases} \frac{dN}{dt} = rN\left(1-\frac{N}{K}\right) - G(N,P)P, \\ \frac{dP}{dt} = \eta G(N,P)P - \gamma P. \end{cases} \tag{1.1}$$

where $N$ and $P$ stand for prey and predator densities, respectively. Here $r > 0$ is the prey intrinsic growth rate, $K$ presents the environmental carrying capacity, the function $G(N, P)$ describes predation known as the functional response, $\eta$ accounts for the efficiency of biomass conversion from predation, and $\gamma$ is the predator's per-capita death rate.

Traditionally, $G(N, P)$ was assumed to depend on the prey population $P$ only, that is, $G(N, P) = g(N)$ where the Holling type (II) is typically adopted for $g(N)$. However, it was found that such a predator–prey

model with *prey-dependent* functional response may face the so-called "paradox of enrichment" [23,35] and the "biological control paradox" [4,30]. There have been efforts in modifying (1.1) with *prey-dependent* functional response $G(N, P) = g(N)$ to avoid the paradoxes. Astrom [9] argued that there need not be any paradox if the linear per capital growth rate of prey is replaced by the nonlinear one $1 - (N/K)^\theta$, where $\theta > 0$ is a species- specific parameter. Deng et al. [18] showed that replacing the constant per-capita death rate $\gamma$ by the density dependent rate $\gamma + sP$ in (1.1) can also get rid of the paradox. The third direction of efforts is to adopt the ratio-dependent functional response by letting $G(N, P) = g(N/P)$ leading to the following ratio-dependent prey–predator system:

$$\begin{cases} \frac{dN}{dt} = rN\left(1 - \frac{N}{K}\right) - \frac{\alpha NP}{P+\alpha\beta N}, \\ \frac{dP}{dt} = \frac{\eta\alpha NP}{P+\alpha\beta N} - \gamma P, \end{cases} \tag{1.2}$$

which was suggested by Arditi and Ginzburg [5]. Here $\alpha$ and $\beta$ are predator's attack rate and handling time, respectively. Since $P/N$ accounts for the relative availability of preys for the predators, such a ratio-dependent predation mechanism may well justify the scenario of those predations when searching for prey is a major portion of predation [1,5,6,14,17]. Model (1.2) has been supported by numerous field and laboratory experiments and observations [1,5,6]. Moreover, theoretical analysis on (1.2) has shown that it can exhibit neither the paradox of enrichment nor the biological control paradox [7,24,25]. As such, ratio-dependent predation is gradually gaining acceptance. There have been a lot of works dedicated to the study of (1.2) and its various variations, which have shown that ratio-dependent predation can support very rich dynamics. See, e.g., [1,5,6,13,20,24–28,36,43–45] and references therein.

On the other hand, it is known that spatial dispersion is an main factor that contributes to the spatial heterogeneity leading to spatial patterns. The importance of spatial models has been recognized by the biologists for a long time and has been one of the dominant themes in both ecology and mathematical ecology [8,22,31,32]. A natural way to incorporate the spatial dispersion into (1.2) is by adding a diffusion term into each of the two equations in (1.2), resulting in the following system of reaction diffusion equations:

$$\begin{cases} \frac{\partial N(x,t)}{\partial t} = d_1 \triangle N(x,t) + rN(x,t)\left(1 - \frac{N(x,t)}{K}\right) \\ \qquad\qquad - \frac{\alpha N(x,t)P(x,t)}{P(x,t)+\alpha\beta N(x,t)}, \\ \frac{\partial P(x,t)}{\partial t} = d_2 \triangle P(x,t) + \frac{\eta\alpha N(x,t)P(x,t)}{P(x,t)+\alpha\beta N(x,t)} - \gamma P(x,t), \end{cases} \tag{1.3}$$

where $d_1$ and $d_2$ are the diffusion rates of the prey and predator, respectively, $x$ is the spatial variable, and $\triangle$ is the Laplancian operator with respect to $x$. For simplicity, let us consider one-dimensional space meaning that $x$ is a scalar, and hence $\triangle N(x,t) = N_{xx}(x,t)$ and $\triangle P(x,t) = P_{xx}(x,t)$. Re-scaling the variables by

$$u = \frac{\alpha\beta}{\eta K} N, \quad v = \frac{\alpha\beta}{\eta^2 K} P, \quad \tilde{t} = \frac{\eta}{\beta} t, \quad \hat{x} = \sqrt{\frac{\eta}{\beta}} x$$

and then dropping the hats, (1.3) is transformed to

$$\begin{cases} \frac{\partial u(x,t)}{\partial t} = d_1 u_{xx}(x,t) + au(x,t)\left(1 - \frac{u(x,t)}{b}\right) \\ \qquad\qquad - \frac{bu(x,t)v(x,t)}{bu(x,t)+v(x,t)}, \\ \frac{\partial v(x,t)}{\partial t} = d_2 v_{xx}(x,t) + \left(\frac{bu(x,t)}{bu(x,t)+v(x,t)} - c\right) v(x,t), \end{cases} \tag{1.4}$$

where

$$a = \frac{r\beta}{\eta}, \quad b = \frac{\alpha\beta}{\eta}, \quad c = \frac{\gamma\beta}{\eta}.$$

Without loss of generality for one-dimensional bounded domains, we consider the interval $[0, \pi]$ for variable $x$ and pose the zero flux boundary condition to represent a closed (isolated) environment:

$$u_x(0,t) = u_x(\pi,t) = v_x(0,t) = v_x(\pi,t) = 0, \quad t \geq 0. \tag{1.5}$$

Typical initial conditions are as follows:

$$u(x,t) = \phi(x,0), \ v(x,t) = \psi(x,0) \geq 0 \ (\not\equiv 0), \quad x \in [0,\pi].$$

The dynamics of system (1.4) with (1.5–1.6) or similar systems has also been recently studied, for example, in [2,10–12,19,33,40]. Aly et al. [2] showed that diffusion-driven instability may occur for such systems giving rise to a spatially inhomogeneous solution of $\cos x$ shape. Self-organized spatial patterns and chaos in the ratio-dependent predator–prey system have been reported by Banerjee [10] and Banerjee and Petrovskii [11]. Bartumeus et al. [12] performed the linear stability analysis and reported diffusion-driven instability. Fan and Li [19] studied the global asymptotic stability of the unique positive constant equilibrium solution for (1.4).

Pang and Wang [33] studied qualitative properties of solutions to this reaction–diffusion system and showed that although the unique positive constant steady state is globally asymptotically stable for the corresponding ODE model, nonconstant positive steady states exist for the PDE version. Wang et al. [40] investigated the spatiotemporal complexity of a ratio-dependent predator–prey system and numerically revealed that the typical dynamics of population densities is the formation of isolated groups and that the spatially extended model not only has more complex dynamic patterns in the space but also allows chaos and spiral waves. However, the conditions for Turing instability in all these works mentioned above are all necessary conditions *only*, and the mechanisms and scenarios of pattern formation remain less studied and poorly understood.

Recently, theoretical studies on the mechanisms of spatiotemporal pattern formation in diffusive predator–prey models have become an area of active research. However, most of such works in the literature deal with models with *prey-dependent* response functional, see [34,39,46,47] and references therein. As far as diffusive *ratio-dependent* prey–predator models go, there is an obvious lack of rigorous analysis on how diffusion rates and other model parameters affect spatiotemporal pattern formation. Such a lack has limited our understanding of the *ratio-dependent* predation mechanism and its impact on biodiversity and spatial patterns. The purpose of this paper is to provide such a rigorous analysis for the diffusive ratio-dependent prey–predator model (1.4). More precisely, we will employ the bifurcation theory to investigate how the diffusion will induce the Turing instability and how other parameters will affect the pattern formation, all analytically. Necessary and sufficient conditions for the occurrence of Turing instability are obtained, and Hopf and pitchfork bifurcations are also investigated in details. To the best of our knowledge, this is the first work to report the pitchfork bifurcation in diffusive predator–prey systems and to determine the stability of spatially inhomogeneous steady state by calculating the related normal form. When Hopf and Turing bifurcations occur simultaneously, the dynamics near the bifurcation point are much richer and the theoretical analysis is more complicated. We leave the detailed study for this case in another paper [37] .

The rest of the paper is organized as follows. In Sect. 2, the local stability of the positive constant equilibrium, Turing instability induced by diffusion, and the existence of Hopf and steady state bifurcations are studied. In Sect. 3, the formulas for determining the direction and stability of Hopf bifurcation and the type of steady state bifurcation are derived by using the normal form theory for partial differential equations. In Sect. 4, some numerical simulations are presented to illustrate and expand the theoretical results. The paper ends by a conclusion section.

## 2 Stability, turing instability and bifurcation analysis

Simple calculations show that system (1.4) has the zero equilibrium $E_0 = (0, 0)$ (total extinction) and the boundary equilibria $E_1 = (b, 0)$ (extinction of predator). It also has a positive constant equilibrium $E^* = (u^*, v^*)$ (coexistence of prey and predator) with

$$u^* = \frac{b(a + (c-1)b)}{a} \quad v^* = \frac{b(1-c)u^*}{c} = \frac{b^2(1-c)(a+(c-1)b)}{ac},$$

provided that following condition holds:

$$\text{(P0)} \quad 0 < c < 1, \quad a > b(1-c).$$

In the following, we assume that the condition $(P0)$ holds so that $u^* > 0$ and $v^* > 0$ and hence $E^*$ is biologically meaningful. We are interested in the stability of the positive equilibrium $E^*$ .

Let

$$f^{(1)}(u, v) = au\left(1 - \frac{u}{b}\right) - \frac{buv}{bu + v},$$
$$f^{(2)}(u, v) = \frac{buv}{bu + v} - cv. \tag{2.1}$$

Then the linearization of (1.4) at the equilibrium $E^*$ is

$$\begin{pmatrix} \frac{\partial u}{\partial t} \\ \frac{\partial v}{\partial t} \end{pmatrix} = d\Delta \begin{pmatrix} u \\ v \end{pmatrix} + A \begin{pmatrix} u \\ v \end{pmatrix}, \tag{2.2}$$

with

$$d\Delta = \begin{pmatrix} d_1\Delta & 0 \\ 0 & d_2\Delta \end{pmatrix}, \quad A = \begin{pmatrix} a_{11} & a_{12} \\ a_{21} & a_{22} \end{pmatrix},$$

where

$$\begin{aligned} a_{11} &= \frac{\partial f^{(1)}}{\partial u}(u^*, v^*) = b(1-c^2) - a, a_{12} \\ &= \frac{\partial f^{(1)}}{\partial v}(u^*, v^*) = -c^2 < 0, \\ a_{21} &= \frac{\partial f^{(2)}}{\partial u}(u^*, v^*) = b(1-c)^2 > 0, a_{22} \\ &= \frac{\partial f^{(2)}}{\partial v}(u^*, v^*) = c(c-1) < 0. \end{aligned} \tag{2.3}$$

Corresponding to the Neumann boundary condition, define the real-valued Sobolev space

$$X = \left\{ (u, v) \in W^{2,2}(0, \pi), \frac{\partial u}{\partial x} = \frac{\partial v}{\partial x} = 0 \text{ at } x = 0, \pi. \right\}.$$

It is well known that the eigenvalues of $d\Delta$ on $X$ are $-d_1k^2$ and $-d_2k^2$, $k \in \mathbb{N}_0 = \{0, 1, 2, \dots\}$, with corresponding normalized eigenfunctions $\beta_k^1$ and $\beta_k^2$, where

$$\beta_k^1(x) = \begin{pmatrix} \gamma_k(x) \\ 0 \end{pmatrix}, \ \beta_k^2(x) = \begin{pmatrix} 0 \\ \gamma_k(x) \end{pmatrix},$$

$$\gamma_k(x) = \frac{\cos(kx)}{\|\cos(kx)\|_{2,2}}, k \in \mathbb{N}_0.$$

Then the normalized eigenfunctions form an normalized orthogonal basis for $X$. In order to study the linear stability of $E^*$, we consider the trial function of the form

$$\begin{pmatrix} u \\ v \end{pmatrix} = \sum_{k=0}^{\infty} \left( p_{k1}\beta_k^1 + p_{k2}\beta_k^2 \right) e^{\lambda t}, \ p_{k1}, p_{k2} \in \mathbb{C}. \tag{2.4}$$

Noting that $\{\beta_k^1(x), \beta_k^2(x)\}$ is an orthogonal basis, we then know that $(u(x,t), v(x,t))^T$ defined by (2.4) is a nontrivial solution of (2.2) if and only if there is a $k \in \mathbb{N}_0$ such that $\lambda$ satisfies

$$\det(\lambda I - M_k - A) = 0, \tag{2.5}$$

where $I$ is the $2 \times 2$ identity matrix, and $M_k = -k^2 \mathrm{diag}(d_1, d_2)$. It follows from (2.5) that the characteristic equation of (2.2) consists of the following sequence of quadratic equations:

$$\Delta_k(\lambda) \triangleq \lambda^2 + T_k\lambda + J_k = 0, \ k \in \mathbb{N}_0, \tag{2.6}$$

where

$$\begin{aligned} T_k &= (d_1+d_2)k^2 - (a_{11}+a_{22}) \\ &= (d_1+d_2)k^2 - b(1-c^2) + a + c(1-c), \\ J_k &= d_1d_2k^4 - (d_1a_{22}+d_2a_{11})k^2 + a_{11}a_{22} - a_{12}a_{21} \\ &= d_1d_2k^4 - \left[ d_1c(c-1) + d_2\left(b(1-c^2) - a\right) \right] k^2 \\ &\quad + c(1-c)[a + b(c-1)]. \end{aligned} \tag{2.7}$$

### 2.1 Hopf and steady state bifurcations

It is well known that $T_k = 0$ and $J_k > 0$ are necessary conditions for Hopf bifurcation to occur. By (2.3) and (2.7), $T_k = 0$ is equivalent to

$$a = a_H(k, b) \triangleq b(1-c^2) - c(1-c) - (d_1+d_2)k^2, \tag{2.8}$$

and $J_k = 0$ is equivalent to

$$\begin{aligned} a = a_T(k, b) &\triangleq \frac{d_2(1-c^2)k^2 + c(1-c)^2}{d_2k^2 + c(1-c)} b \\ &\quad - \frac{d_1d_2k^4 + d_1c(1-c)k^2}{d_2k^2 + c(1-c)}. \end{aligned} \tag{2.9}$$

Combining (2.8) and (2.9), the two lines $a = a_H(k, b)$ and $a = a_T(k, b)$ intersect at

$$b = b_k^* \triangleq \left( 1 + \frac{d_2k^2}{c(1-c)} \right)^2. \tag{2.10}$$

Note that (2.8) is equivalent to

$$b = b_H(k, a) \triangleq \frac{a}{1-c^2} + \frac{c}{1+c} + \frac{(d_1+d_2)k^2}{1-c^2}. \tag{2.11}$$

Clearly, $b_H(k, a) \neq b_H(j, a)$ for $k \neq j$. For fixed $k$, if $b > b_k^*$ and $a = a_H(k, b)$, then Eq. (2.6) has a purely imaginary roots $\pm i\sqrt{J_k}$. To verify the transversality condition, taking $b$ as a parameter and letting $\lambda(b)$ be the root of Eq. (2.6) such that $Re\lambda\,(b_H(k, a)) = 0$, $Im\lambda\,(b_H(k, a)) = \sqrt{J_k}$. Then taking the derivative of both sides of Eq. (2.6) with respect to $b$, we have

$$\left. \frac{dRe\lambda(b)}{db} \right|_{b=b_H(k,a)} = \frac{1-c^2}{2} > 0. \tag{2.12}$$

By (2.8), (2.9), and (2.12), we can define the following straight lines in the $b - a$ plane:

$$H_k : a = a_H(k, b), \ \ b > b_k^*, \ \ k = 0, 1, \dots, \tag{2.13}$$

on which system (1.4) undergoes Hopf bifurcations near the equilibrium $E^*$.

The line $H_0$ corresponds to the case in the absence of diffusion. Notice that under the condition $(P0)$, $J_0 = c(1-c)(a + b(c-1)) > 0$. Thus, when $d_1 = d_2 = 0$, all roots of Eq. (2.6) have negative real parts if and only if $T_0 = -(a_{11} + a_{22}) > 0$, i.e.,

$$a > b(1-c^2) + c(c-1).$$

Thus, in the absence of diffusion, the equilibrium $E^*$ is asymptotically stable for $a > b(1-c^2) + c(c-1)$ and unstable for $a < b(1-c^2) + c(c-1)$.

Summarizing above discussions, we obtain the following theorem.

**Theorem 2.1** *Assume that the condition* $(P0)$ *holds and let the straight lines* $H_k$ *and* $a_T(k,b)$ *in the* $b-a$ *plane be defined by (2.13) and (2.9), respectively.*

*(i) If* $d_1 = d_2 = 0$, *then the positive equilibrium* $E^*$ *is asymptotically stable for* $a > b(1-c^2)+c(c-1)$ *and unstable for* $a < b(1-c^2)+c(c-1)$;

*(ii) System (1.4) undergoes the steady state bifurcation near the positive equilibrium* $E^*$ *at the straight line* $a = a_T(k,b)$;

*(iii) System (1.4) undergoes Hopf bifurcations near the positive equilibrium* $E^*$ *when* $b = b_H(k,a)$. *A family of spatially homogeneous periodic solutions occur on* $H_0$, *and a family of spatially inhomogeneous periodic solutions occur on* $H_k$, $k = 1,2,\ldots$.

*Remark 2.1* At the intersection points of these Hopf and Turing bifurcation lines, the bifurcations with codimension higher than one occur, which is not considered in Theorem 2.1.

## 2.2 Stability and Turing instability

In this subsection, we consider the influence of the diffusion on the stability of the constant equilibrium $E^*$ and investigate the diffusion-induced spatially inhomogeneous steady state. In [38], Turing concluded that the reaction–diffusion model may exhibit spatial patterns under the following two conditions: (1) the equilibrium is linearly stable in the absence of diffusion; and (2) the equilibrium becomes linearly unstable in the presence of diffusion. Such an instability is called a Turing instability or diffusion-driven instability. From (2.7), it is easy to see that $T_k > 0$ if the equilibrium $E^*$ is asymptotically stable in the absence of diffusion. Therefore, if $a > b(1-c^2)+c(c-1)$, then the Turing instability occurs only provided that $J_k < 0$ for some $k \geq 1$, and the diffusion does not change the stability of the constant equilibrium provided that $J_k > 0$ for all $k \in \mathbb{N}_0$.

From (2.3) and (2.7), it is easy to verify that $J_k \geq 0$ is equivalent to $a \geq a_T(k,b)$, where $a_T(k,b)$ is defined by (2.9), that is, $a_T(k,b) = s_1(k)b + s_2(k)$ where

$$s_1(k) = \frac{d_2(1-c^2)k^2 + c(1-c)^2}{d_2k^2 + c(1-c)} > 0,$$

$$s_2(k) = -\frac{d_1d_2k^4 + d_1c(1-c)k^2}{d_2k^2 + c(1-c)} \leq 0.$$

Note that

$$\frac{ds_1(k)}{dk} = \frac{2d_2dc^2(1-c^2)}{\left(d_2k^2 + c(1-c)\right)^2} > 0$$

$$\frac{ds_2(k)}{dk} = -\frac{2d_1d_2^2k^5 + 4d_1d_2c(1-c)k^3 + 2d_1c^2(1-c)^2k}{\left(d_2k^2 + c(1-c)\right)^2} \leq 0.$$

Thus, with respect to $k$, the slope of the straight line $a = a_T(k,b)$ is increasing and the intercept of the straight line $a = a_T(k,b)$ with the $a-$axis is decreasing.

To determine the intersections of the two family of straight lines given by $a = a_T(k,b)$ and $a = a_H(,k,b)$, we solve $a_T(k+1,b) - a_T(k,b) = 0$ for $b$ to obtain

$$b_k = \frac{d_1}{d_2} + \frac{k^2 + (k+1)^2}{c(1-c)}d_1 + \frac{k^2(k+1)^2}{c^2(1-c)^2}d_1d_2. \tag{2.14}$$

In the $b-a$ plane, we call the curve determined by $J_k = 0$ the Turing bifurcation curve (denoted by $\ell$). By (2.14), defining a polygonal line

$$a = \begin{cases} a_T(0,b), & \frac{d_1}{d_2} < b \leq b_0, \\ a_T(k,b), & b_{k-1} < b \leq b_k,\ k = 1,2,\ldots, \end{cases}$$

then the Turing bifurcation curve $\ell$ is formed by a sequence of line segments $\ell_k$ $(k = 1,2,\ldots)$, where

$$\ell_k : a = a_T(k,b),\ \text{for } b_{k-1} < b \leq b_k. \tag{2.15}$$

Notice that $H_0$ intersects with $\ell_0 : a = b(1-c)$ at $b = 1$, and the slope of the line segment $\ell_k$ is less than the Hopf bifurcation lines $H_k$ since

$$\frac{d_2\left(1-c^2\right)k^2 + c(1-c)^2}{d_2k^2 + c(1-c)} = \frac{d_2k^2 + \frac{c(1-c)}{(1+c)}}{d_2k^2 + c(1-c)}\left(1-c^2\right) < (1-c^2).$$

So, if

$$b_0 = \frac{d_1}{d_2} + \frac{d_1}{c(1-c)} \geq 1, \tag{2.16}$$

then the Turing bifurcation curve $\ell$ always lies on the right of the Hopf bifurcation line $H_0$ (see Fig. 1A). By (2.16), it is easy to verify that $b_0 \geq 1$ is equivalent to

$$d_1 \geq d_1^*(c,d_2) \triangleq \frac{c(1-c)}{d_2 + c(1-c)}d_2.$$

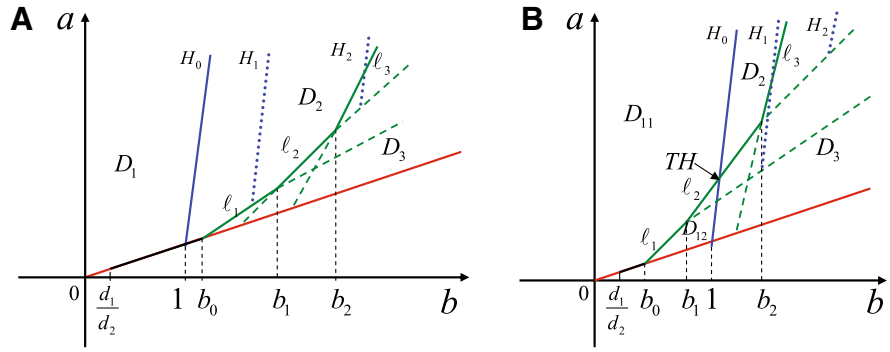


**Fig. 1** Stability region and bifurcation diagram for system (1.4). The region where the positive equilibrium $E^*$ exists is divided into subregions by the real lines $H_i$, $i = 0, 1, 2, \ldots$ and $l_i$, $i = 1, 2, \ldots$, with $H_i$ corresponding to Hopf bifurcations and $l_i$ corresponding Turing bifurcation. **A**: $d_1 \geq d_1^*(c, d_2)$; **B**: $d_1 < d_1^*(c, d_2)$

This implies that the diffusion does not induce the Turing instability if $d_1 \geq d_1^*(c.d_2)$.

If $0 < d_1 < d_1^*(c, d_2)$, the turing bifurcation line $\ell_k$ and Hopf bifurcation line $H_0$ intersect, and there is only one point of intersection since the slope of $\ell_k$ is always less than that of $H_0$. By (2.8) and (2.9), the two lines $H_0$ and $a = a_T(k, b)$ will intersect at

$$b_{HT}(k) = -\frac{d_1 d_2}{c^2(1-c)^2}k^4 - \frac{d_1 - d_2}{c(1-c)}k^2 + 1,$$

which, together with the fact that $k$ is a nonnegative integer, implies that $b_{HT}$ has a maximum at

$$k = k^* = \left[\sqrt{\frac{(d_2 - d_1)c(1-c)}{2d_1 d_2}}\right], \tag{2.17}$$

where $[\cdot]$ is the integer part function. Thus, the line segment $\ell_{k^*}$ and Hopf bifurcation line $H_0$ intersect at $b = b_{HT}(k^*)$.

To figure out the boundary of stability for the positive equilibrium $E^*$, we calculate the rate of change of real root when $b$ increases through the straight line $a = a_T(k, b)$. Solving $J_k = 0$ for $b$, we have

$$b_T(k, a) = \frac{d_2 k^2 + c(1-c)}{d_2\left(1-c^2\right)k^2 + c(1-c)^2}a + \frac{d_1 d_2 k^4 + d_1 c(1-c)k^2}{d_2\left(1-c^2\right)k^2 + c(1-c)^2}. \tag{2.18}$$

Letting $\lambda(b)$ be the real root of the equation $\Delta_k(\lambda) = 0$ such that $\lambda\left(b_T(k, a)\right) = 0$, then it follows from (2.6) and (2.18) that

$$\left.\frac{dRe\lambda(b)}{db}\right|_{b=b_T(k,a)} = \frac{d_2\left(1-c^2\right)k^2 + c(1-c)^2}{T_k}\begin{cases} > 0, & b < b_k^*, \\ < 0, & b > b_k^*, \end{cases} \tag{2.19}$$

where $b_k^*$ is defined by (2.10).

From the above analysis, we obtain the following results on the stability, Turing instability, and steady state bifurcations.

**Theorem 2.2** *Assuming that the condition* $(P0)$ *holds and* $d_1 \geq d_1^*(c, d_2) > 0$. *Then, the diffusion does not affect the stability of the positive equilibrium* $E^*$, *i.e., the stability region* $D_1$ *remains the same as in the case of* $d_1 = d_2 = 0$, *where* $D_1$ *is surrounded by the boundary line for the positive equilibrium* $E^*$, *the Hopf straight line* $H_0$ *and the* $a-$*axis, i.e.,*

$$D_1 = \{(b, a) : 0 < b \leq 1, a > b(1-c)\} \cup \left\{(b, a) : b > 1, a > b(1-c^2) + c(c-1)\right\}.$$

**Theorem 2.3** *Assume that the condition* $(P0)$ *holds,* $0 < d_1 < d_1^*(c, d_2)$, *and let* $\ell_k$ *and* $k^*$ *be defined by (2.15) and (2.17), respectively.*

*(i) When* $(b, a) \in D_{11}$, *the positive equilibrium* $E^*$ *is asymptotically stable for any* $d_1, d_2 \geq 0$, *where* $D_{11}$ *is surrounded by the boundary line for the positive equilibrium* $E^*$, *the Hopf straight line* $H_0$, *the Turing bifurcation polygonal line* $\ell$, *and the* $a-$*axis.*

*(ii) Turing instability occurs in the region* $D_{12}$, *where* $D_{12}$ *is surrounded by the boundary line for the*

*positive equilibrium $E^*$, the Hopf straight line $H_0$, and the Turing bifurcation polygonal line $\ell$.*

*(iii) The Hopf bifurcation line $H_0$ intersects with the line segments $\ell_{k^*}$ and a codimension-2 Turing-Hopf bifurcation occurs at the intersect point $(b, a) = (b_{HT}(k^*), a_{HT}(k^*))$, where*

$$b_{HT}(k^*) = -\frac{d_1 d_2}{c^2(1-c)^2}\left(k^*\right)^4 - \frac{d_1 - d_2}{c(1-c)}\left(k^*\right)^2 + 1,$$

$$a_{HT}(k^*) = (1-c^2)b_{HT}(k^*) + c(c-1).$$

Stability region and bifurcation diagram for system (1.4) are illustrated in Fig. 1. When $d_1 \geq d_2 c(1-c)/\left(d_2 + c(1-c)\right)$, the existence region for the positive equilibrium $E^*$ is divided into three regions $D_1$, $D_2$, and $D_3$, as shown in Fig. 1A. In $D_1$, the positive equilibrium $E^*$ is asymptotically stable. This stability region $D_1$ is the same to the case in the absence of diffusion. However, when $d_1 < d_2 c(1-c)/\left(d_2 + c(1-c)\right)$, the stability region $D_1$ in the absence of diffusion is split into two regions $D_{11}$ and $D_{12}$, as shown in Fig. 1B. In $D_{11}$, the positive equilibrium $E^*$ is still asymptotically stable in the presence of diffusion. In $D_{12}$, Turing instability occurs, and steady state bifurcation occurs. In $D_2$, only Hopf bifurcations occur. In $D_3$, there exist Hopf and steady state bifurcations.

*Remark 2.2* If $k$ in (2.9) is assumed to be nonnegative real number, then the envelope curve of these straight lines $a = a_T(k, b)$ is defined by

$$a = b(1-c^2) + \frac{d_1}{d_2}c(1-c) - 2c(1-c)\sqrt{\frac{d_1}{d_2}b},$$

$$b > \frac{d_1}{d_2},$$

which is the necessary condition for the occurrence of Turing instability. This condition can also be obtained by the results in [2,10,11]. The steady state bifurcation straight lines $\ell_k$, $k = 1, 2, \ldots$, are tangent to this envelope curve.

## 3 Normal form on the center manifold and the properties of Hopf and steady state bifurcations

From Theorem 2.1, we know that system (1.4) may undergo Hopf bifurcations or steady state bifurcation near the equilibrium $E^*$ when $b$ is increasing across the critical curves $H_k$ or $a = a_T(k)$, respectively. Taking $b$ as a parameter, denote the critical value $b$ by $b_*$. Then, $b_* = b_H(k)$ defined by (2.11) for Hopf bifurcations and $b_* = b_T(k)$ defined by (2.18) for steady state bifurcation. In this section, we employ the similar method as in [21] to compute the normal form on the center manifold corresponding to these bifurcations and then determine the properties of these bifurcations.

For $U_1 = (u_1, v_1)^T, U_2 = (u_2, v_2)^T \in X$, define the inner product

$$[U_1, U_2] = \int_0^\pi (u_1 u_2 + v_1 v_2)\, dx$$

such that $X$ becomes a Hilbert space.

Introduce a new parameter $\mu \in \mathbb{R}$ by setting $\mu = b - b_*$ such that $\mu = 0$ is the bifurcation value. Rewrite the positive equilibrium as a parameter-dependent form $E^*_\mu(u^*(\mu), v^*(\mu))$ with

$$u^*(\mu) = \frac{(b_* + \mu)\left(a + (c-1)\left(b_* + \mu\right)\right)}{a},$$

$$v^*(\mu) = \frac{(b_* + \mu)^2 (1-c)(a + (c-1)\left(b_* + \mu\right))}{ac}.$$

Setting $\tilde{u}(\cdot, t) = u(\cdot, t) - u^*(\mu)$, $\tilde{v}(\cdot, t) = v(\cdot, t) - v^*(\mu)$, $\tilde{U}(t) = (\tilde{u}(\cdot, t), \tilde{v}(\cdot, t))$ and then dropping the tildes for simplification of notation, system (1.4) can be written as the equation

$$\frac{dU}{dt} = d\Delta U + L_0(U) + f(U, \mu), \tag{3.1}$$

where

$$d\Delta u = \begin{pmatrix} d_1 \Delta u \\ d_2 \Delta v \end{pmatrix}, L_0(U) = \begin{pmatrix} \left(b_*\left(1-c^2\right) - a\right)u - c^2 v \\ b_*(1-c)^2 u - c(1-c)v \end{pmatrix},$$

$$f(U, \mu) = \sum_{i+j+m \geq 2} \frac{1}{i!j!m!} f_{ijm} u^i v^j \mu^m, \tag{3.2}$$

$$f_{ijm} = \left(f^{(1)}_{ijm}, f^{(2)}_{ijm}\right)^T,$$

with $f^{(n)}_{ijm} = \frac{\partial^{i+j+m} \widetilde{f}^{(n)}(0,0,0)}{\partial u^i \partial v^j \partial \mu^m}$, $n = 1, 2$, and

$$\widetilde{f}^{(1)}(u, v, \mu) = a\left(u + u^*(\mu)\right)\left(1 - \frac{(u + u^*(\mu))}{(b_* + \mu)}\right) - \frac{(b_* + \mu)\left(u + u^*(\mu)\right)\left(v + v^*(\mu)\right)}{(b_* + \mu)\left(u + u^*(\mu)\right) + \left(v + v^*(\mu)\right)},$$

$$\widetilde{f}^{(2)}(u, v, \mu) = \frac{(b_* + \mu)\left(u + u^*(\mu)\right)\left(v + v^*(\mu)\right)}{(b_* + \mu)\left(u + u^*(\mu)\right) + \left(v + v^*(\mu)\right)} - c\left(v + v^*(\mu)\right).$$

By a direct computation, we have $f_{011} = f_{002} = f_{003} = f_{012} = f_{102} = (0,0)^T$, which will be used in the following computation.

The linearized system of Eq. (3.1) at the origin is

$$\frac{dU}{dt} = \mathscr{L}(U). \tag{3.3}$$

Denote by $\Lambda_k$ the finite set of all eigenvalues of the linearized system (3.3) having zero real parts, with which a stable invariant manifold is associated. Set $\mathscr{B}_k = \text{span}\left\{\left[\varphi(\cdot), \beta_k^i\right]\beta_k^i | \ \varphi \in X, i = 1,2\right\}$. Then it is easy to verify that

$$L_0(\mathscr{B}_k) \subset \text{span}\left\{\beta_k^1, \beta_k^2\right\}, k \in \mathbb{N}_0.$$

Assume that $y(t) \in \mathbb{R}^2$ and

$$y^T(t)\begin{pmatrix}\beta_k^1\\ \beta_k^2\end{pmatrix} \in \mathscr{B}_k.$$

Then, on $\mathscr{B}_k$, the linear partial differential Eq. (3.3) is equivalent to the ODE on $\mathbb{R}^2$

$$\dot{y}(t) = \begin{pmatrix}-d_1k^2 & 0\\ 0 & -d_2k^2\end{pmatrix} y(t) + L_0(y(t)), \tag{3.4}$$

where for $y(t) \in \mathbb{R}^2$, we use the same formal expression $L_0(y(t))$ as in (3.2). Clearly, the linear ordinary differential Eq. (3.4) has the same characteristic Eq. (2.6) as the linear partial differential Eq. (3.3).

Let

$$\mathcal{M}_k = \begin{pmatrix}-d_1k^2 + b_*\left(1-c^2\right) - a & -c^2\\ b_*(1-c)^2 & -d_2k^2 - c(1-c)\end{pmatrix}, \tag{3.5}$$

be the characteristic matrix of Eq. (3.4). Then $\Lambda_k$ is the finite set of all eigenvalues of the matrix (3.5) having zero real parts. The standard adjoint theory for ODEs can be used to decompose $\mathbb{C}^2$ by $\Lambda_k$ as

$$\mathbb{C}^2 = P_k \oplus Q_k,$$

where $P_k$ is the generalized eigenspace associated with the eigenvalues in $\Lambda_k$ and

$$Q_k = \left\{\varphi \in \mathbb{C}^2 : \ < \psi, \varphi >= 0 \text{ for all } \psi \in P_k^*\right\},$$

where $P_k^*$ is the dual space of $P_k$, and $< \cdot, \cdot >$ is the scalar product of two complex vectors defined by

$$\left\langle \psi^T, \varphi \right\rangle = \psi^T\varphi, \text{ for } \varphi, \psi \in \mathbb{C}^2,$$

such that for dual bases $\Phi_k$ and $\Psi_k$ of $P_k$ and $P_k^*$, respectively, $< \Psi_k, \Phi_k >= I_p$, where $p = dim P_k$.

Using the above decomposition, the phase space $X$ can be decomposed as

$$X = X^c \oplus X^s, \ X^c = \text{Im}\pi, \ X^s = \text{Ker}\pi, \tag{3.6}$$

where $\dim X^c = p$, and $\pi : X \to X^c$ is the projection defined by

$$\pi(\phi) = \left(\Phi_k \left\langle \Psi_k, \begin{pmatrix}\left[\phi, \beta_k^1\right]\\ \left[\phi, \beta_k^2\right]\end{pmatrix}\right\rangle\right)^T \begin{pmatrix}\beta_k^1\\ \beta_k^2\end{pmatrix}, \ \phi \in X.$$

According to (3.6), $U = (u, v)^T \in X$ can be decomposed as

$$\begin{pmatrix}u\\ v\end{pmatrix} = (\Phi_k z)^T \begin{pmatrix}\beta_k^1\\ \beta_k^2\end{pmatrix} + w = \Phi_k z \gamma_k(x) + w, \tag{3.7}$$

where $z = (z_1, z_2)^T \in \mathbb{R}^p$, $w = (w_1, w_2)^T \in X^s$. Then, system (3.1) is equivalent to the following system:

$$\begin{cases}\dot{z} = B_k z + \Psi_k \begin{pmatrix}\left[f(z,w,\mu), \beta_k^1\right]\\ \left[f(z,w,\mu), \beta_k^2\right]\end{pmatrix},\\ \dot{w} = \mathscr{L}(w) + H(z,w,\mu),\end{cases} \tag{3.8}$$

where $B_k$ is a $p \times p$ real diagonal matrix with the point spectrum $\sigma(B_k) = \Lambda_k$,

$$f(z,w,\mu) = f\left(\Phi_k z \gamma_k(x) + w, \mu\right) \tag{3.9}$$

and

$$H(z,w,\mu) = f(z,w,\mu) - \left(\Phi_k \left\langle \Psi_k, \begin{pmatrix}\left[f(z,w,\mu), \beta_k^1\right]\\ \left[f(z,w,\mu), \beta_k^2\right]\end{pmatrix}\right\rangle\right)^T \begin{pmatrix}\beta_k^1\\ \beta_k^2\end{pmatrix}. \tag{3.10}$$

Consider the formal Taylor expansion

$$f(\varphi, \mu) = \sum_{j\geq 2} \frac{1}{j!} f_j(\varphi, \mu),$$

where $f_j$ is the $j$th Fréchet derivative of $f$. Then (3.8) is written as

$$\begin{cases}\dot{z} = B_k z + \sum_{j\geq 2} \frac{1}{j!} f_j^1(z,w,\mu),\\ \dot{w} = \mathscr{L}(w) + \sum_{j\geq 2} \frac{1}{j!} f_j^2(z,w,\mu),\end{cases} \tag{3.11}$$

where

$$\begin{aligned} f_j^1(z,w,\mu) &= \Psi_k \begin{pmatrix}\left[f_j(z,w,\mu), \beta_k^1\right]\\ \left[f_j(z,w,\mu), \beta_k^2\right]\end{pmatrix},\\ f_j^2(z,w,\mu) &= H_j(z,w,\mu).\end{aligned} \tag{3.12}$$

As for autonomous ODEs in the finite dimension space [16], by a recursive transformation of variables

$$(z,w)=(\widetilde{z},\widetilde{w})+\frac{1}{j!}\left(U_j^1(\widetilde{z},\mu),U_j^2(\widetilde{z},\mu)\right),\ j\geq 2,$$

where $U_j^1$ and $U_j^2$ are homogeneous polynomials of degree $j$ in $\widetilde{z}$ and $\mu$, and for simplification of notation, dropping the tilde after each transformation of variable, then the normal form on the center manifold for 3.8 (or (3.11)) is

$$\dot{z}=B_k z+\frac{1}{2}g_2^1(z,0,\mu)+\frac{1}{3!}g_3^1(z,0,\mu)+o(\mu|z|^2). \tag{3.13}$$

where $g_2^1$ and $g_3^1$ are the second and third terms in $(z,\mu)$, respectively, given by

$$\begin{aligned} g_2^1(z,0,\mu)&=\mathrm{Proj}_{\mathrm{Ker}(M_2^1)}f_2^1(z,0,\mu),\ g_3^1(z,0,\mu)\\ &=\mathrm{Proj}_{\mathrm{Ker}(M_3^1)}\tilde{f}_3^1(z,0,\mu). \end{aligned} \tag{3.14}$$

Here, $\frac{1}{3!}\tilde{f}_3^1$ is the term of order 3 obtained after the changes of variables in previous step given by

$$\begin{aligned} \tilde{f}_3^1(z,0,\mu)=&f_3^1(z,0,\mu)\\ &+\frac{3}{2}\left[\left(D_z f_2^1\right)(z,0,\mu)U_2^1(z,\mu)\right.\\ &+\left(D_w f_2^1\right)(z,0,\mu)U_2^2(z,\mu)\\ &\left.-\left(D_z U_2^1(z,\mu)\right)g_2^1(z,0,\mu)\right], \end{aligned} \tag{3.15}$$

and the operators $M_j^1$ and $M_j^2$ are defined by

$$\begin{aligned} &M_j^1:V_j^{p+1}\left(\mathbb{C}^2\right)\to V_j^{p+1}\left(\mathbb{C}^2\right),M_j^1\left(U_j^1\right)\\ &=\left(D_z U_j^1(z,\mu)B_k z\right)-B_k U_j^1(z,\mu),\\ &M_j^2:V_j^{p+1}\left(X^s\right)\to V_j^{p+1}\left(X^s\right),M_j^2\left(U_j^2\right)\\ &=\left(D_z U_j^2(z,\mu)B_k z\right)-\mathscr{L}(U_j^2(z,\mu)), \end{aligned} \tag{3.16}$$

where $V_j^{p+1}(Y)$ denotes the space of homogeneous polynomials of degree $j$ in $p+1$ variables $z_1,z_2,\ldots,z_p,\mu$ with coefficients in $Y$.

## 3.1 For Hopf bifurcations: direction and stability of Hopf bifurcations

We assume that there exists a $k\in\mathbb{N}_0$ such that $\Delta_k=0$ with $b=b_*=b_H(k)$ has a pair of purely imaginary roots $\pm i\omega_k$ and the remaining roots of the characteristic equation (2.6) have nonzero real parts, where

$$\omega_k=\sqrt{d_1d_2k^4-\left(d_1c(c-1)+d_2\left(b_*(1-c^2)-a\right)\right)k^2+c(1-c)(a+b_*(c-1))}.$$

For this Hopf bifurcation, we have $\Lambda_k=\{i\omega_k,-i\omega_k\}$, $p=2$, $B_k=\mathrm{diag}\{i\omega_k,-i\omega_k\}$, and $z=(z_1,z_2)^T\in\mathbb{R}^2$.

In terms of $\mathcal{M}_k p_k=i\omega_k p_k$ and $\mathcal{M}_k^T q_k=i\omega_k q_k$, we can choose $p_k$ and $q_k$ as follows such that $\langle q_k^T,p_k\rangle=1$,

$$p_k=\begin{pmatrix}1\\ -\frac{d_1k^2-b_*(1-c^2)+a+i\omega_k}{c^2}\end{pmatrix},$$

$$q_k=\begin{pmatrix}\frac{d_2k^2+c(1-c)+i\omega_k}{2i\omega_k}\\ -\frac{c^2}{2i\omega_k}\end{pmatrix}.$$

Define $\Phi_k=(p_k,\bar{p}_k)$, $\Psi_k=col\left(q_k^T,\bar{q}_k^T\right)$ and then $\langle\Psi_k,\Phi_k\rangle=\Psi_k\Phi_k=I_2$, where $I_2$ is the $2\times 2$ identity matrix. Then, by (3.7), we use the following decomposition in this subsection:

$$\begin{aligned} &\begin{pmatrix}u\\ v\end{pmatrix}=(z_1p_k+z_2\bar{p}_k)\gamma_k(x)+w,z_1,z_2\in\mathbb{R},\\ &w=(w_1,w_2)^T\in X^s. \end{aligned} \tag{3.17}$$

By (3.16) and noticing that $B_k=\mathrm{diag}\{i\omega_k,-i\omega_k\}$, the operators $M_j^1$ are defined by

$$\begin{aligned} &M_j^1\left(z_1^{m_1}z_2^{m_2}\mu^m e_n\right)\\ &=i\omega_k\left(m_1-m_2+(-1)^n\right)z_1^{m_1}z_2^{m_2}\mu^m e_n,\\ &m_1+m_2+m=j, \end{aligned}$$

for $m_1,m_2,m\in\mathbb{N}_0$, $n=1,2$, $j=2,3$, and $e_1=(1,0)^T$, $e_2=(0,1)^T$. Hence,

$$\mathrm{Im}(M_2^1)^c=\mathrm{Ker}(M_2^1)=\mathrm{span}\left\{\begin{pmatrix}z_1\mu\\ 0\end{pmatrix},\begin{pmatrix}0\\ z_2\mu\end{pmatrix}\right\},$$

and

$$\begin{aligned} &\mathrm{Im}(M_3^1)^c=\mathrm{Ker}(M_3^1)\\ &=\mathrm{span}\left\{\begin{pmatrix}z_1^2z_2\\ 0\end{pmatrix},\begin{pmatrix}z_1\mu^2\\ 0\end{pmatrix}\begin{pmatrix}0\\ z_1z_2^2\end{pmatrix}\begin{pmatrix}0\\ z_2\mu^2\end{pmatrix}\right\}. \end{aligned}$$

### 3.1.1 Calculation of $g_2^1(z,0,\mu)$

By (3.2) and a direct computation, we have $f_{101}=\left(1-c^2,(1-c)^2\right)^T$. So,

$$\begin{aligned} \frac{1}{2}f_2(U,\mu)=&\begin{pmatrix}1-c^2\\ (1-c)^2\end{pmatrix}\mu u+\frac{1}{2}f_{200}u^2\\ &+f_{110}uv+\frac{1}{2}f_{020}v^2. \end{aligned} \tag{3.18}$$

which, together with (3.17), leads to

$$\begin{aligned}\frac{1}{2}f_2(z,0,\mu)&=\frac{1}{2}f_2\left(\Phi_k z\gamma_k(x),0\right)\\&=\begin{pmatrix}1-c^2\\(1-c)^2\end{pmatrix}\left(p_{k1}z_1\mu+\bar{p}_{k1}z_2\mu\right)\gamma_k(x)\\&\quad+\frac{1}{2}\left(A_{k20}z_1^2+A_{k11}z_1z_2+A_{k02}z_2^2\right)\gamma_k^2(x),\end{aligned}\tag{3.19}$$

where

$$\begin{aligned}A_{k20}&=f_{200}p_{k1}^2+2f_{110}p_{k1}p_{k2}+f_{020}p_{k2}^2,\\A_{k02}&=\bar{A}_{k20},\\A_{k11}&=2f_{200}\left|p_{k1}\right|^2+4f_{110}\mathrm{Re}\left\{p_{k1}\bar{p}_{k2}\right\}\\&\quad+2f_{020}\left|p_{k2}\right|^2.\end{aligned}\tag{3.20}$$

Thus, from (3.12) and (3.19), we obtain

$$\frac{1}{2}g_2^1(z,0,\mu)=\frac{1}{2}\mathrm{Proj}_{\mathrm{Ker}(M_2^1)}f_2^1(z,0,\mu)=\begin{pmatrix}B_{k1}z_1\mu\\\bar{B}_{k1}z_2\mu\end{pmatrix},\tag{3.21}$$

where

$$B_{k1}=\left(\left(1-c^2\right)q_{k1}+(1-c)^2q_{k2}\right)p_{k1}.\tag{3.22}$$

*3.1.2 Calculation of $g_3^1(z,0,\mu)$*

Notice that the terms $o(|z|\mu^2)$ are irrelevant to determine the generic Hopf bifurcation. So, it is sufficient for determining the dynamics of generic Hopf bifurcation to obtain $g_3^1(z,0,0)$. Since $g_2^1(z,0,0)=0$, it follows from (3.15) that the third term $g_3^1(z,0,0)$ can be determined as follows:

$$\frac{1}{3!}g_3^1(z,0,0)=\frac{1}{3!}\mathrm{Proj}_S\tilde{f}_3^1(z,0,0),$$

where

$$S=\mathrm{span}\left\{\begin{pmatrix}z_1^2z_2\\0\end{pmatrix},\begin{pmatrix}0\\z_1z_2^2\end{pmatrix}\right\}$$

and

$$\begin{aligned}\tilde{f}_3^1(z,0,0)&=f_3^1(z,0,0)+\frac{3}{2}\Big[(D_zf_2^1)(z,0,0)U_2^1(z,0)\\&\quad+(D_wf_2^1)(z,0,0)U_2^2(z,0)\Big].\end{aligned}\tag{3.23}$$

Here,

$$U_2^1(z,0)=(M_2^1)^{-1}\mathrm{Proj}_{\mathrm{Im}(M_2^1)}f_2^1(z,0,0)\tag{3.24}$$

and $U_2^2(z,0)$ is determined by the equation

$$\left(M_2^2U_2^2\right)(z,0)=f_2^2(z,0,0).\tag{3.25}$$

Next we compute the third-order term $g_3^1(z,0,0)=\mathrm{Proj}_S\tilde{f}_3^1(z,0,0)$ step by step in terms of (3.23).

**Step 1.** The calculation of $\mathrm{Proj}_Sf_3^1(z,0,0)$. By (3.2) and (3.12) and notice that

$$\int_0^\pi\gamma_k^4(x)dx=\begin{cases}\frac{1}{\pi},&k=0,\\\frac{3}{2\pi},&k\neq0,\end{cases}$$

it is easy to verify that

$$\frac{1}{3!}\mathrm{Proj}_Sf_3^1(z,0,0)=\begin{pmatrix}B_{k21}z_1^2z_2\\\bar{B}_{k21}z_1z_2^2\end{pmatrix},\tag{3.26}$$

where

$$B_{k21}=\begin{cases}\frac{1}{2\pi}b_{k21},&k=0,\\\frac{3}{4\pi}b_{k21},&k\neq0,\end{cases}\tag{3.27}$$

with

$$\begin{aligned}b_{k21}&=q_k^T\Big(f_{300}p_{k1}\left|p_{k1}\right|^2+f_{030}p_{k2}\left|p_{k2}\right|^2\\&\quad+f_{210}\left(p_{k1}^2\bar{p}_{k2}+2p_{k2}\left|p_{k1}\right|^2\right)\\&\quad+f_{120}\left(p_{k2}^2\bar{p}_{k1}+2p_{k1}\left|p_{k2}\right|^2\right)\Big).\end{aligned}\tag{3.28}$$

**Step 2.** The calculation of $\mathrm{Proj}_S\Big[\left(D_zf_2^1\right)(z,0,0)U_2^1(z,0)\Big]$. It follows from (3.12) and (3.19) that

$$\begin{aligned}f_2^1(z,0,0)&=\Psi_k\left(A_{k20}z_1^2+A_{k11}z_1z_2+A_{k02}z_2^2\right)\\&\quad\times\int_0^\pi\gamma_k^3(x)dx,\end{aligned}$$

A straightforward calculation shows that

$$\begin{aligned}U_2^1(z,0)&=(M_2^1)^{-1}f_2^1(z,0,0)\\&=\frac{\int_0^\pi\gamma_k^3(x)dx}{i\omega_k}\begin{pmatrix}q_k^T\left(A_{k20}z_1^2-A_{k11}z_1z_2-\frac{1}{3}A_{k02}z_2^2\right)\\\bar{q}_k^T\left(\frac{1}{3}A_{k20}z_1^2+A_{k11}z_1z_2-A_{k02}z_2^2\right)\end{pmatrix},\end{aligned}$$

and then

$$\frac{1}{3!}\mathrm{Proj}_S[(D_zf_2^1)U_2^1](z,0,0)=\begin{pmatrix}C_{k21}z_1^2z_2\\\bar{C}_{k21}z_1z_2^2\end{pmatrix},\tag{3.29}$$

with

$$C_{k21}=\begin{cases}\frac{1}{6\pi}c_{k21},&k=0,\\0,&k\neq0,\end{cases}\tag{3.30}$$

where

$$c_{k21}=\frac{i}{\omega_k}\left(\left(q_k^T A_{k20}\right)\left(q_k^T A_{k11}\right)-\left|q_k^T A_{k11}\right|^2-\frac{2}{3}\left|q_k^T A_{k02}\right|^2\right). \tag{3.31}$$

**Step 3.** The calculation of $\mathrm{Proj}_S\left[\left(D_w f_2^1\right)(z,0,0)\,U_2^2(z,0)\right]$. Let

$$U_2^2(z,0): h=\sum_{j\geq 0}(h_{kj}(z))^T\begin{pmatrix}\beta_j^1\\ \beta_j^2\end{pmatrix}\in X^s, \tag{3.32}$$

with

$$h_{kj}(z)=\begin{pmatrix}h_{kj}^{(1)}(z)\\ h_{kj}^{(2)}(z)\end{pmatrix}=\begin{pmatrix}h_{kj20}^{(1)}\\ h_{kj20}^{(2)}\end{pmatrix}z_1^2+\begin{pmatrix}h_{kj11}^{(1)}\\ h_{kj11}^{(2)}\end{pmatrix}z_1z_2+\begin{pmatrix}h_{kj02}^{(1)}\\ h_{kj02}^{(2)}\end{pmatrix}z_2^2.$$

From (3.12), we have

$$\begin{aligned}&\left(D_w f_2^1\right)(z,0,0)(h)\\&=\Psi_k\begin{pmatrix}\left[Df_2\left(\Phi_k z\gamma_k(x),0\right)\left(h_{kk}^T\begin{pmatrix}\beta_k^1\\ \beta_k^2\end{pmatrix}\right),\beta_k^1\right]\\ \left[Df_2\left(\Phi_k z\gamma_k(x),0\right)\left(h_{kk}^T\begin{pmatrix}\beta_k^1\\ \beta_k^2\end{pmatrix}\right),\beta_k^2\right]\end{pmatrix}\\&+\Psi_k\begin{pmatrix}\left[Df_2\left(\Phi_k z\gamma_k(x),0\right)\left(\sum_{j\neq k}h_{kj}^T\begin{pmatrix}\beta_j^1\\ \beta_j^2\end{pmatrix}\right),\beta_k^1\right]\\ \left[Df_2\left(\Phi_k z\gamma_k(x),0\right)\left(\sum_{j\neq k}h_{kj}^T\begin{pmatrix}\beta_j^1\\ \beta_j^2\end{pmatrix}\right),\beta_k^2\right]\end{pmatrix}.\end{aligned}$$

By (3.18) and a direct computation, we obtain

$$\begin{aligned}&\begin{pmatrix}\left[Df_2\left(\Phi_k z\gamma_k(x),0\right)\left(h_{kj}^T\begin{pmatrix}\beta_j^1\\ \beta_j^2\end{pmatrix}\right),\beta_k^1\right]\\ \left[Df_2\left(\Phi_k z\gamma_k(x),0\right)\left(h_{kj}^T\begin{pmatrix}\beta_j^1\\ \beta_j^2\end{pmatrix}\right),\beta_k^2\right]\end{pmatrix}\\&=2c_{kj}\left\{f_{200}\left(z_1p_{k1}+z_2\bar{p}_{k1}\right)h_{kj}^{(1)}\right.\\&+f_{110}\left(\left(z_1p_{k2}+z_2\bar{p}_{k2}\right)h_{kj}^{(1)}\right.\\&\left.\left.+\left(z_1p_{k1}+z_2\bar{p}_{k1}\right)h_{kj}^{(2)}\right)+f_{020}\left(z_1p_{k2}+z_2\bar{p}_{k2}\right)h_{kj}^{(2)}\right\},\end{aligned}$$

where

$$c_{kj}=\int_0^\pi\gamma_k^2(x)\gamma_j(x)dx=\begin{cases}\frac{1}{\sqrt{\pi}}, & j=k=0,\\ \frac{1}{\sqrt{\pi}}, & j=0,k\neq 0,\\ \frac{1}{\sqrt{2\pi}}, & j=2k\neq 0,\\ 0, & \text{otherwise.}\end{cases} \tag{3.33}$$

So,

$$\frac{1}{3!}\mathrm{Proj}_S\left(D_w f_2^1\right)(z,0,0)(h)=\begin{pmatrix}D_{k21}z_1^2z_2\\ \bar{D}_{k21}z_1z_2^2\end{pmatrix} \tag{3.34}$$

with

$$D_{k21}=\begin{cases}\frac{1}{3\sqrt{\pi}}E_{(0,0)}, & k=0,\\ \frac{1}{3\sqrt{\pi}}E_{(k,0)}+\frac{1}{3\sqrt{2\pi}}E_{(k,2k)}, & k\neq 0,\end{cases}$$

where, for $j=0,2k$,

$$\begin{aligned}E_{(k,j)}=q_k^T\left(\right.&\left(f_{200}p_{k1}+f_{110}p_{k2}\right)h_{kj11}^{(1)}\\&+\left(f_{110}p_{k1}+f_{020}p_{k2}\right)h_{kj11}^{(2)}\\&+\left(f_{200}\bar{p}_{k1}+f_{110}\bar{p}_{k2}\right)h_{kj20}^{(1)}\\&\left.+\left(f_{110}\bar{p}_{k1}+f_{020}\bar{p}_{k2}\right)h_{kj20}^{(2)}\right).\end{aligned} \tag{3.35}$$

Clearly, to obtain $D_{k21}$ we still need to compute $h_{kj20}$ and $h_{kj11}$. It follows from (3.16) that

$$\begin{aligned}&M_2^2\left((h_{kj}(z))^T\begin{pmatrix}\beta_j^1\\ \beta_j^2\end{pmatrix}\right)\\&=\left(D_z\left((h_{kj}(z))^T\begin{pmatrix}\beta_j^1\\ \beta_j^2\end{pmatrix}\right)B_kz\right)\\&\quad-\mathscr{L}\left((h_{kj}(z))^T\begin{pmatrix}\beta_j^1\\ \beta_j^2\end{pmatrix}\right),\end{aligned}$$

which leads to

$$\begin{aligned}&\begin{pmatrix}\left[M_2^2\left((h_{kj}(z))^T\begin{pmatrix}\beta_j^1\\ \beta_j^2\end{pmatrix}\right),\beta_j^1\right]\\ \left[M_2^2\left((h_{kj}(z))^T\begin{pmatrix}\beta_j^1\\ \beta_j^2\end{pmatrix}\right),\beta_j^2\right]\end{pmatrix}\\&=2i\omega_k\left(h_{kj20}z_1^2-h_{kj02}z_2^2\right)\\&\quad+j^2\begin{pmatrix}d_1&0\\0&d_2\end{pmatrix}h_{kj}(z)-L_0h_{kj}(z).\end{aligned} \tag{3.36}$$

In addition, by (3.10) and (3.12) we have

$$\begin{aligned}&H(z,w,\mu)\\&=f(z,w,\mu)-\left\langle q_k^T,\begin{pmatrix}\left[f(z,w,\mu),\beta_k^1\right]\\ \left[f(z,w,\mu),\beta_k^2\right]\end{pmatrix}\right\rangle p_k\gamma_k(x)\\&\quad-\left\langle\bar{q}_k^T,\begin{pmatrix}\left[f(z,w,\mu),\beta_k^1\right]\\ \left[f(z,w,\mu),\beta_k^2\right]\end{pmatrix}\right\rangle\bar{p}_k\gamma_k(x),\end{aligned}$$

which, together with (3.12) and (3.19), yields

$$\begin{aligned}\begin{pmatrix}\left[f_2^2(z,0,0),\beta_j^1\right]\\ \left[f_2^2(z,0,0),\beta_j^2\right]\end{pmatrix} &= \begin{pmatrix}\left[H_2(z,0,0),\beta_j^1\right]\\ \left[H_2(z,0,0),\beta_j^2\right]\end{pmatrix}\\ &= \sum_{m_1+m_2=2}\left(c_{kj}A_{km_1m_2}\right.\\ &\quad\left.-\zeta_{kj}\left(q_k^TA_{km_1m_2}p_k+\bar{q}_k^TA_{km_1m_2}\bar{p}_k\right)\right)z_1^{m_1}z_2^{m_2}.\end{aligned} \tag{3.37}$$

where $\zeta_{kj}=\int_0^\pi\gamma_k^3(x)dx\int_0^\pi\gamma_k(x)\gamma_j(x)dx$.

From (3.25), we have

$$\begin{pmatrix}\left[M_2^2\left((h_{kj}(z))^T\begin{pmatrix}\beta_j^1\\ \beta_j^2\end{pmatrix}\right),\beta_j^1\right]\\ \left[M_2^2\left((h_{kj}(z))^T\begin{pmatrix}\beta_j^1\\ \beta_j^2\end{pmatrix}\right),\beta_j^2\right]\end{pmatrix}=\begin{pmatrix}\left[f_2^2,\beta_j^1\right]\\ \left[f_2^2,\beta_j^2\right]\end{pmatrix}.$$

So, by (3.36), (3.37) and matching the coefficients of $z_1^2$ and $z_1z_2$, we have

$$\begin{aligned}z_1^2:\quad &2i\omega_kh_{kj20}+j^2\begin{pmatrix}d_1&0\\0&d_2\end{pmatrix}h_{kj20}-L_0\left(h_{kj20}\right)\\ &=\left(c_{kj}A_{k20}-\zeta_{kj}\left(q_k^TA_{k20}p_k+\bar{q}_k^TA_{k20}\bar{p}_k\right)\right),\\ z_1z_2:\quad &j^2\begin{pmatrix}d_1&0\\0&d_2\end{pmatrix}h_{kj11}-L_0\left(h_{kj11}\right)\\ &=\left(c_{kj}A_{k11}-\zeta_{kj}\left(q_k^TA_{k11}p_k+\bar{q}_k^TA_{k11}\bar{p}_k\right)\right),\end{aligned}$$

Solving these equations yields

$$k=0,\ j=0:\begin{cases}h_{0020}=\frac{1}{\sqrt{\pi}}\left(2i\omega_0I_2-\mathcal{M}_0\right)^{-1}\\ \quad\left(A_{020}-q_0^TA_{020}p_0-\bar{q}_0^TA_{020}\bar{p}_0\right),\\ h_{0011}=-\frac{1}{\sqrt{\pi}}\mathcal{M}_0^{-1}\\ \quad\left(A_{011}-q_0^TA_{011}p_0-\bar{q}_0^TA_{011}\bar{p}_0\right),\end{cases}$$

and

$$k\neq0,\ j=0,2k:\begin{cases}h_{kj20}=c_{kj}\left(2i\omega_kI_2-\mathcal{M}_j\right)^{-1}A_{k20},\\ h_{kj11}=-c_{kj}\mathcal{M}_j^{-1}A_{k11}.\end{cases}$$

Summarizing Steps 1–3 and by (3.26), (3.29) and (3.34), we obtain

$$\frac{1}{3!}g_3^1(z,0,0)=\frac{1}{3!}\mathrm{Proj}_S\tilde{f}_3^1(x,0,0)=\begin{pmatrix}B_{k2}z_1^2z_2\\ \bar{B}_{k2}z_1z_2^2\end{pmatrix}$$

with

$$\begin{aligned}B_{k2}&=B_{k21}+\frac{3}{2}\left(C_{k21}+D_{k21}\right)\\ &=\begin{cases}\frac{1}{2\pi}b_{021}+\frac{1}{4\pi}c_{021}+\frac{1}{2\sqrt{\pi}}E_{(0,0)}, & k=0,\\ \frac{3}{4\pi}b_{k21}+\frac{1}{2\sqrt{\pi}}E_{k,0}+\frac{1}{2\sqrt{2\pi}}E_{(k,2k)}, & k\neq0,\end{cases}\end{aligned} \tag{3.38}$$

where $b_{k21}$, $c_{k21}$, and $E_{(k,j)}$ are defined by (3.28), (3.31), and (3.35), respectively.

Thus, the normal form (3.13) on the center manifold for the critical values $b=b_H(k)$ of Hopf bifurcations has the form

$$\begin{aligned}\dot{z}&=B_kz+\begin{pmatrix}B_{k1}z_1\mu\\ \bar{B}_{k1}z_2\mu\end{pmatrix}+\begin{pmatrix}B_{k2}z_1^2z_2\\ \bar{B}_{k2}z_1z_2^2\end{pmatrix}\\ &\quad+O(|z|\mu^2+|z^4|),\end{aligned}$$

which can be written in real coordinates $w$ through the change of variables $z_1=w_1-iw_2$, $z_2=w_1+iw_2$. Transforming to polar coordinates $w_1=\rho\cos\xi$, $w_2=\rho\sin\xi$, this normal form becomes

$$\begin{aligned}\dot{\rho}&=\nu_{k1}\mu\rho+\nu_{k2}\rho^3+O(\mu^2\rho+|(\mu,\rho)|^4),\\ \dot{\xi}&=-\omega_k+O(|(\mu,\rho)|)\end{aligned} \tag{3.39}$$

with

$$\nu_{k1}=\mathrm{Re}\left\{B_{k1}\right\}=\frac{1-c^2}{2}>0,\ \ \nu_{k2}=\mathrm{Re}\left\{B_{k2}\right\}.$$

It is well known [29,42] that the sign of $\nu_{k1}\nu_{k2}$ determines the direction of the bifurcation (supercritical if $\nu_{k1}\nu_{k2}<0$, subcritical if $\nu_{k1}\nu_{k2}>0$), and the sign of $\nu_{k2}$ determines the stability of the nontrivial periodic orbits (stable if $\nu_{k2}<0$, unstable if $\nu_{k2}>0$). Since $\nu_{k1}>0$, then the direction and stability of the Hopf bifurcation at $b=b_H^k$ can be determined by the sign of $\nu_{k2}$.

**Theorem 3.1** *Assume that there exists a $k\in\mathbb{N}_0$ such that $\Delta_k=0$ with $b=b_*=b_H(k)$ has a pair of purely imaginary roots $\pm i\omega_k$, and the remaining roots of the characteristic equation (2.6) have nonzero real parts. Let $b_H(k)$ and $B_{k2}$ be defined by (2.11) and (3.38), respectively.*

*(i) If $Re\{B_{k2}\}<0$, then the Hopf bifurcation at the critical value $b_H(k)$ is supercritical, and the bifurcating periodic solution is asymptotically stable on the center manifold.*

*(ii) If $Re\{B_{k2}\}>0$, then the Hopf bifurcation at the critical value $b_H(k)$ is subcritical, and the bifurcating periodic solution is unstable on the center manifold.*

### 3.2 For the steady state bifurcation: pitchfork bifurcation and stability

In this subsection, we assume that there exists a positive integer $k\geq1$ such that $\Delta_k=0$ with $b=b_*=b_T(k)$

has a simple zero root $\lambda = 0$ and the remaining roots of the characteristic Eq. (2.6) have nonzero real parts.

For this singularity, we have that $\Lambda_k = \{0\}$, $p = 1$, $B_k = 0$, $\Phi_k = p_k$, $\Psi_k = q_k^T$ with

$$p_k = \begin{pmatrix} 1 \\ -\frac{d_1k^2 - b_*(1-c^2)+a}{c^2} \end{pmatrix}, \quad q_k = \begin{pmatrix} \frac{d_2k^2+c(1-c)}{T_k} \\ -\frac{c^2}{T_k} \end{pmatrix}.$$

Then, by (3.7), we use the following decomposition in this subsection:

$$\begin{pmatrix} u \\ v \end{pmatrix} = p_k z\gamma_k(x) + w, z \in \mathbb{R}, \ w = (w_1, w_2)^T \in X^s. \tag{3.40}$$

It follows from (3.18) and (3.40) that

$$\begin{aligned} \frac{1}{2} f_2(z, 0, \mu) &= \frac{1}{2} f_2 \left(p_k z\gamma_k(x), \mu\right) \\ &= \begin{pmatrix} 1 - c^2 \\ (1-c)^2 \end{pmatrix} p_{k1}\gamma_k(x) z\mu \\ &\quad + \frac{1}{2} A_{k20}\gamma_k^2(x) z^2, \end{aligned} \tag{3.41}$$

where $A_{k20}$ has the same form as in (3.20). Since $B_k = 0$, it is easy to see from (3.16) that $\mathrm{Im}(M_j^1)$ is the zero subspace of $V_j^2(\mathbb{R})$, and then we have

$$\begin{aligned} \mathrm{Im}(M_2^1)^c &= \mathrm{span}\left\{z^2, z\mu, \mu^2\right\}, \ \mathrm{Im}(M_3^1)^c \\ &= \mathrm{span}\left\{z^3, z^2\mu, z\mu^2, \mu^3\right\}. \end{aligned} \tag{3.42}$$

From (3.12), (3.41), and (3.42), the second-order term $g_2^1$ of the normal form is given by

$$\begin{aligned} \frac{1}{2} g_2^1(z, 0, \mu) &= \frac{1}{2} \mathrm{Proj}_{\mathrm{Im}(M_2^1)^c} f_2^1(z, 0, \mu) \\ &= S_{k11} z\mu + S_{k21} z^2, \end{aligned} \tag{3.43}$$

where

$$\begin{aligned} S_{k11} &= \left(\left(1 - c^2\right) q_{k1} + (1-c)^2 q_{k2}\right) p_{k1} \\ &= \frac{(1-c)\left(c(1-c) + d_2(1+c)\right)}{T_k} > 0 \end{aligned} \tag{3.44}$$

and

$$S_{k21} = \int_0^\pi \gamma_k^3(x) dx q_k^T A_{k20} = 0.$$

In what follows, we compute the third terms of the normal form for determining the steady state bifurcation. Since $B = 0$, it is easy to see that $(\mathrm{Ker}(M_3^1))^c = 0$ and then $U_2^1 = 0$. By (3.43), we know that $g_2^1(z, 0, 0) = 2S_{k21} z^2 = 0$.

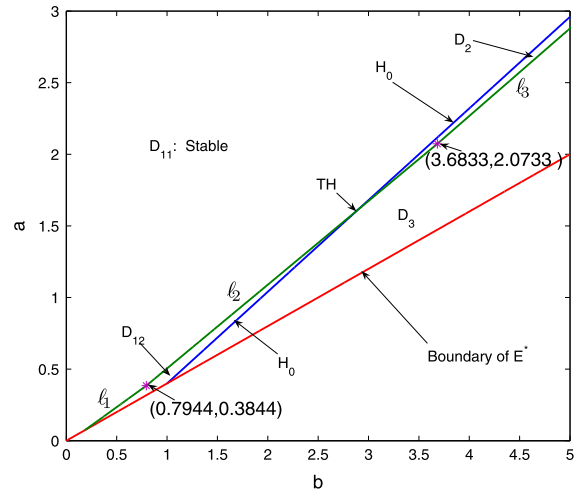


**Fig. 2** Bifurcation diagram for system (1.4) with $d_1 = 0.02$, $d_2 = 0.2$, $c = 0.6$, in the $b - a$ plane. The positive equilibrium $E^*$ is asymptotically stable in $D_{11}$ and unstable otherwise. In $D_{12}$, Turing instability occurs. In $D_2$, only Hopf bifurcations occur. In $D_3$, there exist Hopf and steady state bifurcations

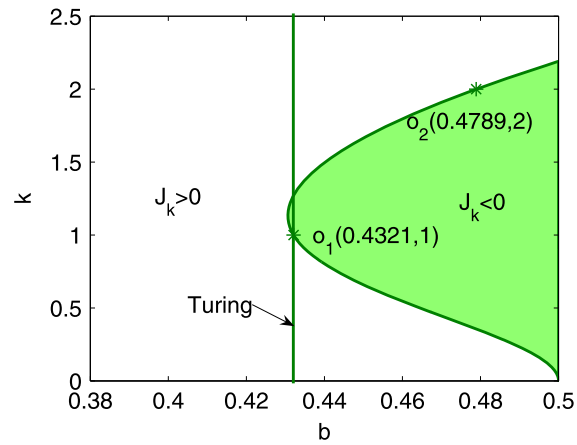


**Fig. 3** Bifurcation diagram for system (1.4) in the $b - k$ plane for fixed $a = 0.2$: bifurcation occurs at $b = b_* = 0.4321$ when $k = 1$, and at $b = b_* = 0.4789$ when $k = 2$. Parameters $d_1$, $d_2$, and $c$ are the same as in Fig. 2: $d_1 = 0.02$, $d_2 = 0.2$, $c = 0.6$

It follows from (3.23) and (3.42) that

$$\frac{1}{3!} g_3^1(z, 0, \mu) = \frac{1}{3!} \mathrm{Proj}_S \widetilde{f}_3^1(z, 0, 0) + O(\mu|(z, \mu)|^2),$$

where $S = \mathrm{span}\left\{z^3\right\}$.

Let

$$U_2^2(z, 0) : h = \sum_{j \geq 0} \left( \begin{pmatrix} h_{kj}^{(1)} \\ h_{kj}^{(2)} \end{pmatrix} z^2 \right)^T \begin{pmatrix} \beta_j^1 \\ \beta_j^2 \end{pmatrix} \in X^s, \tag{3.45}$$

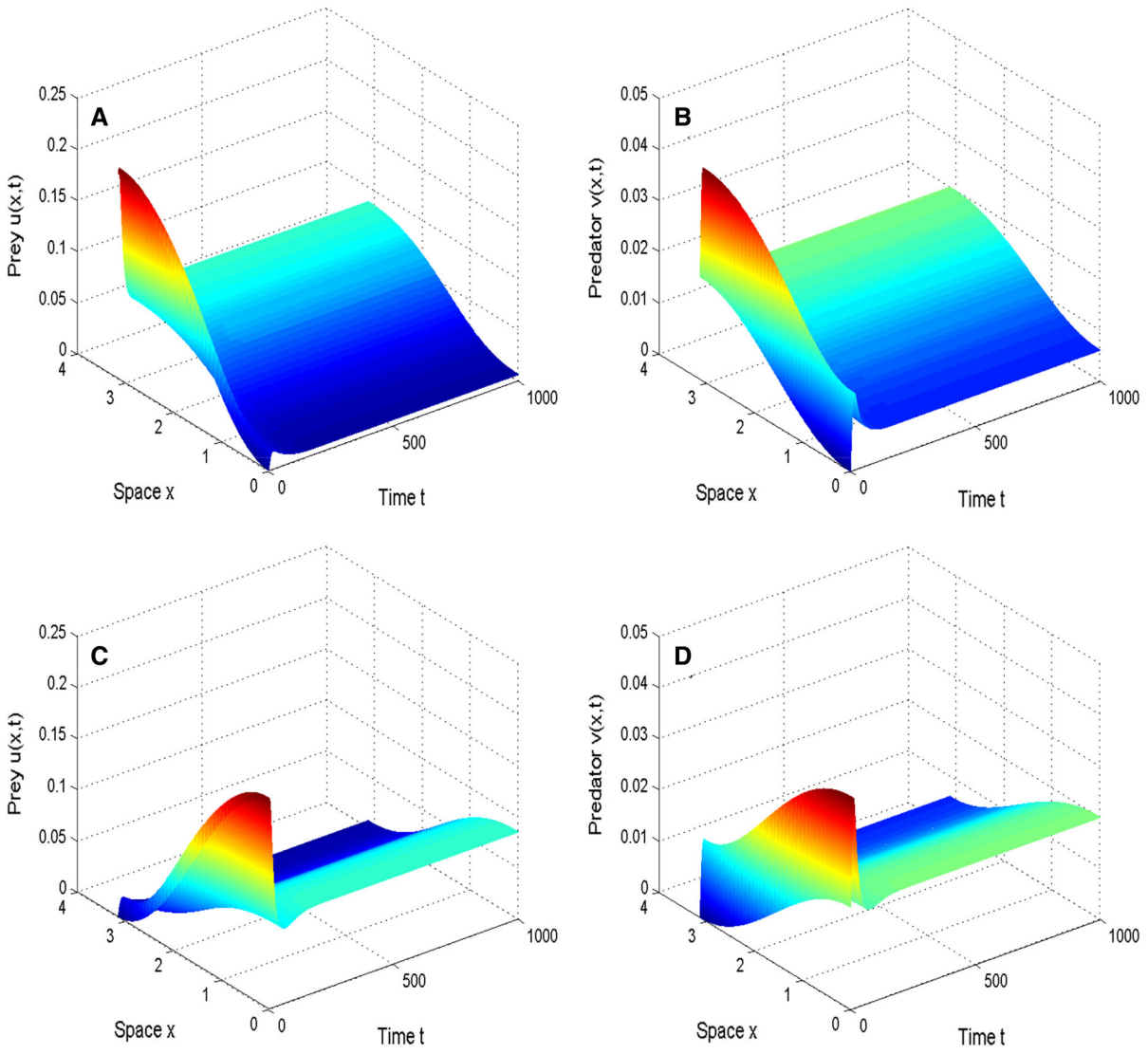


**Fig. 4** Pitchfork bifurcation of positive constant equilibrium: $d_1 = 0.02, d_2 = 0.2, c = 0.6, a = 0.2, b = 0.46$. The positive constant equilibrium $E^*(0.0368, 0.0113)$ is unstable, and two stable spatially inhomogeneous steady states of $\cos x$-like shape emerge and are stable. **a**–**b** The initial values are $u(x, 0) = 0.1 - 0.1\cos x$, $v(x, 0) = 0.01 - 0.01\cos x$; **c**–**d** The initial values are $u(x, 0) = 0.1 + 0.1\cos x$, $v(x, 0) = 0.01 + 0.01\cos x$

where $h_{kj}^{(1)}, h_{kj}^{(2)} \in \mathbb{R}$. By (3.2), (3.12), and (3.15), we have

$$\frac{1}{3!}\mathrm{Proj}_S \tilde{f}_3^1(z, 0, 0) = S_{k30} z^3,$$

where

$$S_{k30} = \frac{1}{4\pi} s_k + \frac{1}{2\sqrt{\pi}} s_{(k,0)} + \frac{1}{2\sqrt{2\pi}} s_{(k,2k)}, \qquad (3.46)$$

with

$$\begin{aligned} s_k &= q_k^T \left( f_{300} p_{k1}^3 + f_{030} p_{k2}^3 + 3 f_{210} p_{k1}^2 p_{k2} \right. \\ &\quad \left. + 3 f_{120} p_{k1} p_{k2}^2 \right), \\ s_{(k,j)} &= q_k^T \left( (f_{200} p_{k1} + f_{110} p_{k2}) h_{kj}^{(1)} + (f_{020} p_{k2} \right. \\ &\quad \left. + f_{110} p_{k1}) h_{kj}^{(2)} \right), \quad j = 0, 2k. \end{aligned} \qquad (3.47)$$

Clearly, to obtain $S_{k30}$, we have to determine $h_{kj}$. Using the similar arguments as for Hopf bifurcation, it

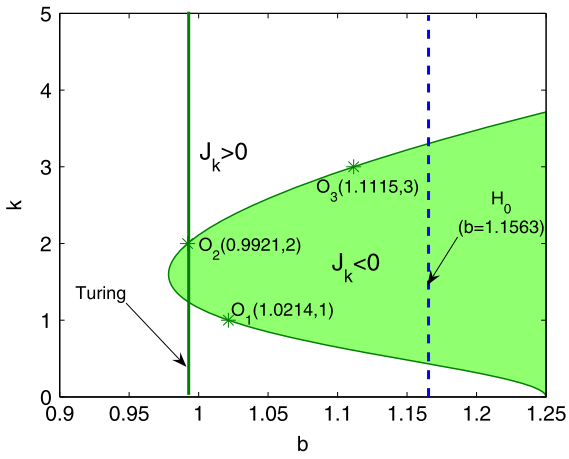


**Fig. 5** Bifurcation diagram for system (1.4) in the $b-k$ plane for $a = 0.5$. Other parameters $d_1$, $d_2$ and $c$ are same as in Fig. 2

is easy to show that $h_{kj}$ satisfy

$$-\mathcal{M}_j h_{kj} = c_{kj} A_{k20},\ k \neq 0,\ j = 0,\ 2k. \tag{3.48}$$

Using the basic assumption of this subsection, we know that $\det(\mathcal{M}_j) \neq 0$ for $k \neq 0$, $j = 0, 2k$. Therefore, by (3.48), we obtain

$$h_{kj} = -c_{kj}\mathcal{M}_j^{-1} A_{k20},\ k \neq 0,\ j = 0,\ 2k. \tag{3.49}$$

Now, the coefficient $S_{k30}$ can be explicitly determined by (3.46), (3.47) and (3.49). Thus, if $S_{k30} \neq 0$, then the normal form truncated to third terms is given by

$$\dot{z} = S_{k11} z\mu + S_{k30} z^3, \tag{3.50}$$

where $S_{k11}$ and $S_{k30}$ are defined by (3.44) and (3.46), respectively. Therefore, by the center manifold theorem due to Carr [15] and the bifurcation theorem [16,29], the dynamics of system (1.4) near the bifurcation value is topologically equivalent to that of normal form near the sufficiently small neighborhood of $\mu = 0$. Notice that $S_{k11} > 0$. So, by the normal form (3.50) and the results of [41], we have the following results on the steady state bifurcation.

**Theorem 3.2** *Assume that there exists a positive integer $k$ such that $\Delta_k = 0$ with $b = b_T(k)$ has a simple zero root $\lambda = 0$, and the remaining roots of the characteristic equation (2.6) have nonzero real parts. Let $b_T(k)$ and $S_{k30}$ be defined by (2.18) and (3.46), respectively. Then we have the following results on the steady state bifurcation:*

*(i) if $S_{k30} < 0$, then system (1.4) undergoes a supercritical pitchfork bifurcation near the constant equilibrium $E^*$ at the critical value $b = b_T(k)$;*

*(ii) if $S_{k30} > 0$, then system (1.4) undergoes a subcritical pitchfork bifurcation near the constant equilibrium $E^*$ at the critical value $b = b_T(k)$;*

## 4 Numerical simulations

The formulas obtained in Sects. 2 and 3 are complicated but can be numerically evaluated. In this section, we present some numerical results for these formulas and numerical simulations for the models system. These numeric results confirm our analytic results.

For numerical purpose, we take $d_1 = 0.02, d_2 = 0.2, c = 0.6$ so that

$$d_1 < (d_2 c(1-c))/(d_2 + c(1-c)).$$

By $(P0)$, the positive equilibrium $E^*$ exists provided that $a > 0.4b$. It follows from (2.9), (2.13), and (2.15) that

$$H_0:\ a = \frac{16}{25}b - \frac{6}{25},\ b > 1;$$
$$\ell_1:\ a = \frac{28}{55}b - \frac{1}{50},\ \frac{11}{60} < b \leq \frac{143}{180};$$
$$\ell_2:\ a = \frac{38}{65}b - \frac{2}{25},\ \frac{143}{180} < b \leq \frac{221}{60};$$
$$\ell_3:\ a = \frac{52}{85}b - \frac{9}{50},\ \frac{221}{60} < b \leq \frac{731}{60},$$

and the straight line $H_0$ intersects with $\ell_2$ at the point $TH\left(\frac{26}{9}, \frac{362}{225}\right)$. Figure 2 shows the stability region and these bifurcation lines in the $b-a$ plane.

In the sequel, we will fix $a$ and take $b$ as a parameter and observe how the dynamics of system (1.4) changes as $b$ varies.

Depending on whether system (1.4) first undergoes Hopf bifurcation or steady state bifurcation, we distinguish the following two cases.

### 4.1 Pitchfork bifurcations and spatially inhomogeneous steady states

For $a \in (0.0733, 1.6089)$, system (1.4) first undergoes steady state bifurcation as $b$ increases. The interval $(0.0733, 1.6089)$ further breaks down into $(0.0733, 0.3844)$ and $(0.3844), 1.6089)$, corresponding to steady state bifurcations with different spatial patterns.

**4.1-(i).** Spatially inhomogeneous steady states with $\cos x$-like shape.

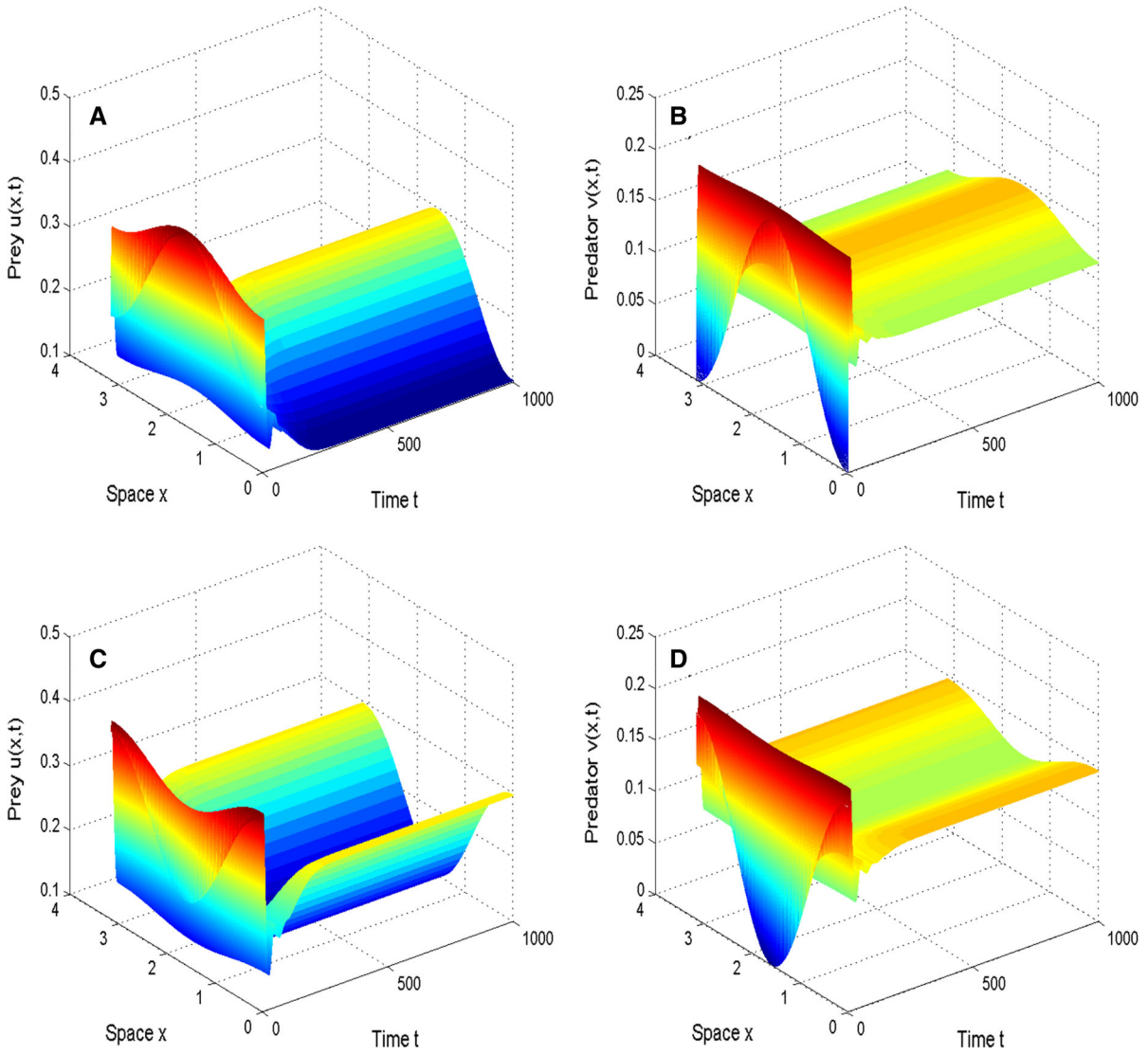


**Fig. 6** Numerical simulation of system (1.4) for $d_1 = 0.02, d_2 = 0.2, a = 0.5, b = 1.02, c = 0.6$. The positive equilibrium $E^*(0.1877, 0.1276)$ is unstable and two spatially inhomogeneous stable steady states like $\cos 2x$ shape emerge. **a**–**b**: The initial values are $u(x, 0) = 0.3 - 0.1\cos x$, $v(x, 0) = 0.1 - 0.1\cos x$; **c**–**d** The initial values are $u(x, 0) = 0.3 + 0.1\cos x$, $v(x, 0) = 0.1 + 0.1\cos x$

When $a \in (0.0733, 0.3844)$, steady state bifurcation occurs when $b$ increasingly crosses the Turing bifurcation **line** $\ell_1$. Taking $a = 0.2$ as an example, Fig. 3 illustrates the bifurcation diagram in the $b - k$ plane. The positive equilibrium $E^*$ is asymptotically stable for $0 < b < 0.4321$ and unstable for $0.4321 < b < 0.5$. It follows from Fig. 3 that when $b$ increases from 0 to 0.5, system (1.4) undergoes steady state bifurcation at the $O_1$ when $k = 1$ or at $O_2$ when $k = 2$, and there is no Hopf bifurcation. At $b = 0.4321$, $J_1 = 0$, and $J_k > 0$ for $k > 1$; thus, the characteristic equation $\Delta_1 = 0$ has a zero root $\lambda = 0$, and all other roots of $\Delta_k = 0$ with $k > 1$ have negative real parts. By (3.50) and taking advantage of Matlab, we can calculate the normal form truncated to the third- order term at the critical value $b = 0.4321$ of steady state as

$$\dot{z} = 0.5842z\mu + 0.2359z^3.$$

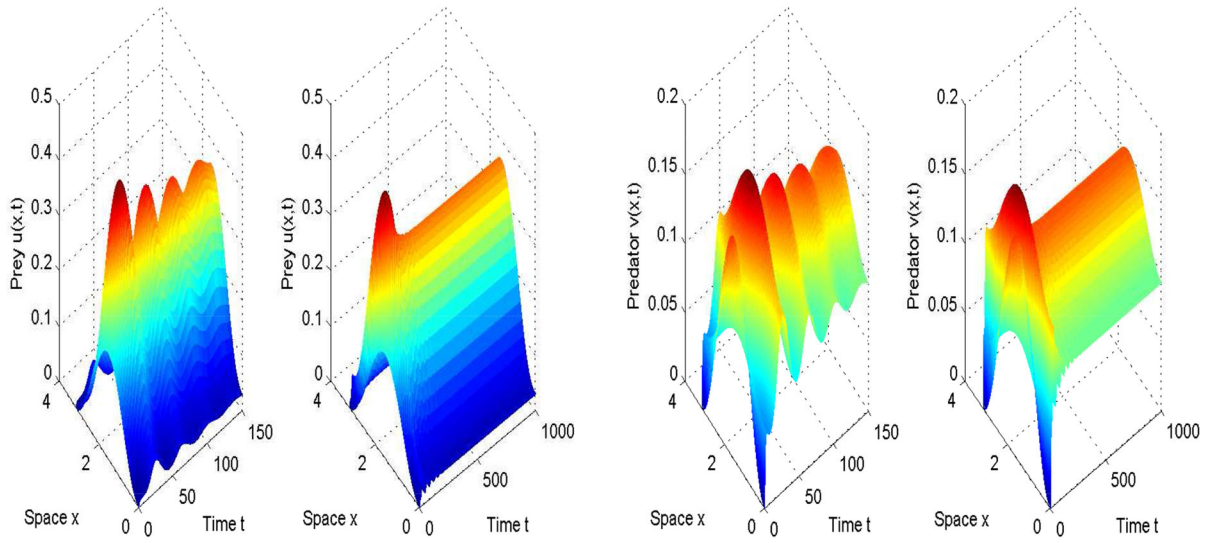


**Fig. 7** Numerical simulation of system (1.4) for $d_1 = 0.02, d_2 = 0.2, a = 0.5, b = 1.6, c = 0.6$. The positive equilibrium $E^*(0.0835, 0.0640)$ is unstable and a spatial homogeneous Hopf bifurcation occurs. This Hopf bifurcating periodic solution is unstable. The initial values are $u(x, 0) = 0.1 - 0.1\cos(2x)$, $v(x, 0) = 0.08 - 0.08\cos(2x)$

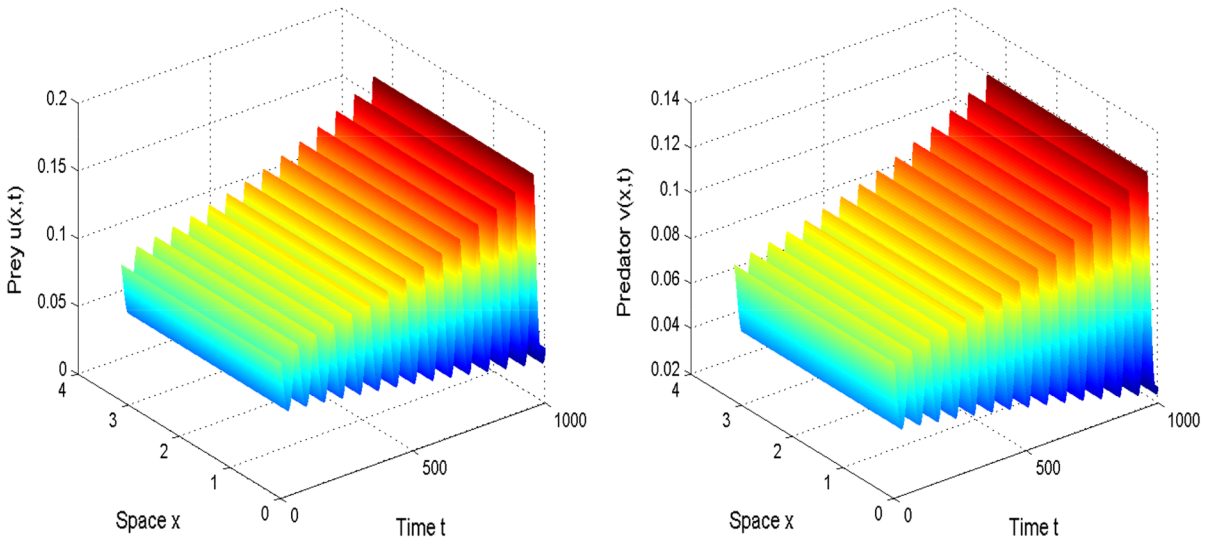


**Fig. 8** Numerical simulation of system (1.4). The parameters $d_1, d_2, a, b, c$ are the same as Fig. 7. But here we take the spatial homogeneous initial values $u(x, 0) = 0.1$, $v(x, 0) = 0.08$

By Theorem 3.2, we conclude that system (1.4) undergoes a subcritical pitchfork bifurcation at $b = 0.4321$, meaning that there is a sufficiently small positive number $\varepsilon^*$ such that for any $b \in (0.4321 - \varepsilon^*, 0.4321)$, there exist two unstable spatially inhomogeneous steady states with $\cos x$-like shape. We would like to point out that for $b$ greater than and sufficiently close to the critical value 0.4321, numerical simulation shows that there exist two spatially inhomogeneous steady states of $\cos x$-like shape, which are *stable* now, as shown in Fig. 4 for $b = 0.46$.

**4.1-(ii).** Spatially inhomogeneous stable steady states with like $\cos 2x$ shape.

When $a \in (0.3844, 1.6089)$, steady state bifurcation occurs when $b$ increasingly crosses the Turing bifurcation **line** $\ell_2$. Taking $a = 0.5$, Fig. 5 illustrates the bifurcation diagram in the $b - k$ plane. At the point $O_k, k = 1, 2, 3, J_k = 0$, and system (1.4) under-

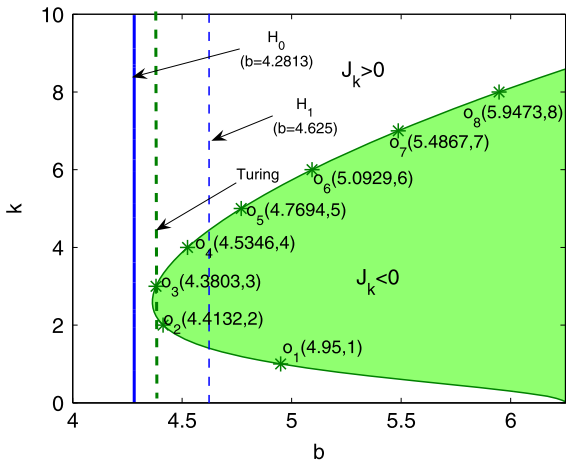


**Fig. 9** Bifurcation diagram for system (1.4) in the $b-k$ plane for fixed $a = 2.5$ such that $b$ first increases across $H_0$. Other parameters $d_1$, $d_2$, and $c$ are same as in Fig. 2

goes steady state bifurcation. It follows from Fig. 5 and (2.19) that when $b < 0.9921$, all roots of the characteristic Eq. (2.6) for any $k \in \mathbb{N}_0$ have negative real parts, and thus, the positive equilibrium $E^*$ is asymptotically stable. When $b = 0.9921$, the equation $\Delta_2 = 0$ has a zero root $\lambda = 0$ and a negative real root, while all roots of $\Delta_k = 0$ with $k \neq 2$ all have negative real parts. When $b > 0.9921$, the characteristic equation $\Delta_2 = 0$ has at least one positive real root, and the positive equilibrium $E^*$ becomes unstable.

By using Matlab, we can calculate the normal form (3.50) at the critical value $b = 0.9921$ truncated to the third-order term as

$$\dot{z} = 0.6172z\mu - 0.6374z^3,$$

which implies that system (1.4) undergoes a supercritical pitchfork bifurcation at $b = 0.9921$. Taking $b = 1.02$, Fig. 6 shows that the positive equilibrium $E^*(0.1877, 0.1276)$ is unstable, and two spatially inhomogeneous stable steady states of $\cos 2x$-like shape emerge. Although the steady state bifurcations occur at $O_1$ and $O_3$, they must be unstable since $\Delta_2 = 0$ has a positive real root for $b > 0.9921$.

From Fig. 5, we also can see that system (1.4) undergoes a spatially homogeneous Hopf bifurcation at $b = 1.1563$. By (3.39) and using the software Matlab, we can compute the following normal form truncated to the third-order term:

$$\dot{\rho} = 0.3200\mu\rho - 0.0257\rho^3,$$

which implies, (by Theorem 3.2 ), that the Hopf bifurcation at $b = 1.1563$ is supercritical and stable on the center manifold. However, since $\Delta_k = 0$ $(k = 1, 2, 3)$ have positive real roots at $b = 1.1563$, these bifurcated spatially homogeneous periodic solutions are unstable in the whole phase space. Figures 7 and 8 illustrate this unstable Hopf bifurcation for spatially dependent initial values and constant initial values, respectively.

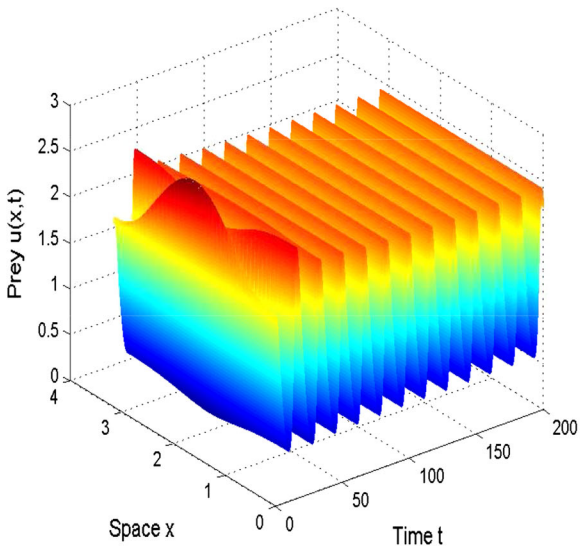


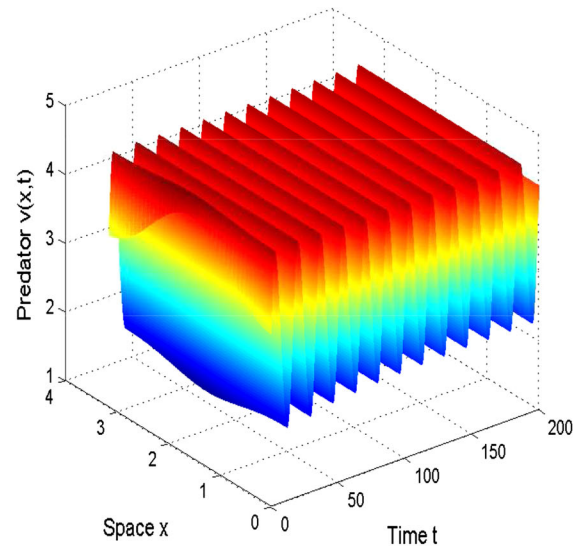


**Fig. 10** Numerical simulation of system (1.4) for $d_1 = 0.02, d_2 = 0.2, a = 2.5, b = 4.3, c = 0.6$. The positive equilibrium $E^*(1.3416, 3.8459)$ is unstable, and there exists a spatially homogenous stable periodic orbit. The initial values are $u(x, 0) = 2.5 - 0.5\cos 2x$, $v(x, 0) = 4 - 0.5\cos 2x$

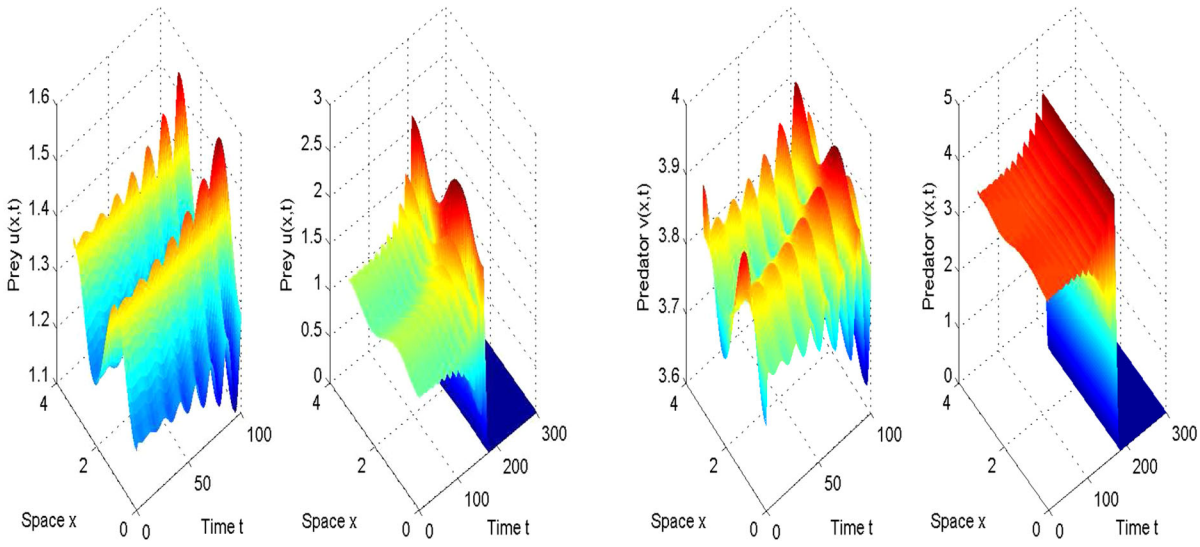


**Fig. 11** Numerical simulation of system (1.4) for $d_1 = 0.02, d_2 = 0.2, a = 2.5, b = 4.39, c = 0.6$. The positive equilibrium $E^*(1.3065, 3.8236)$ is unstable, and an unstable steady state solution like $\cos 3x$ shape emerges. Finally, the system evolves into the zero solution. The initial values are $u(x, 0) = 1.3065 - 0.1\cos 3x$, $v(x, 0) = 3.8236 - 0.1\cos 3x$

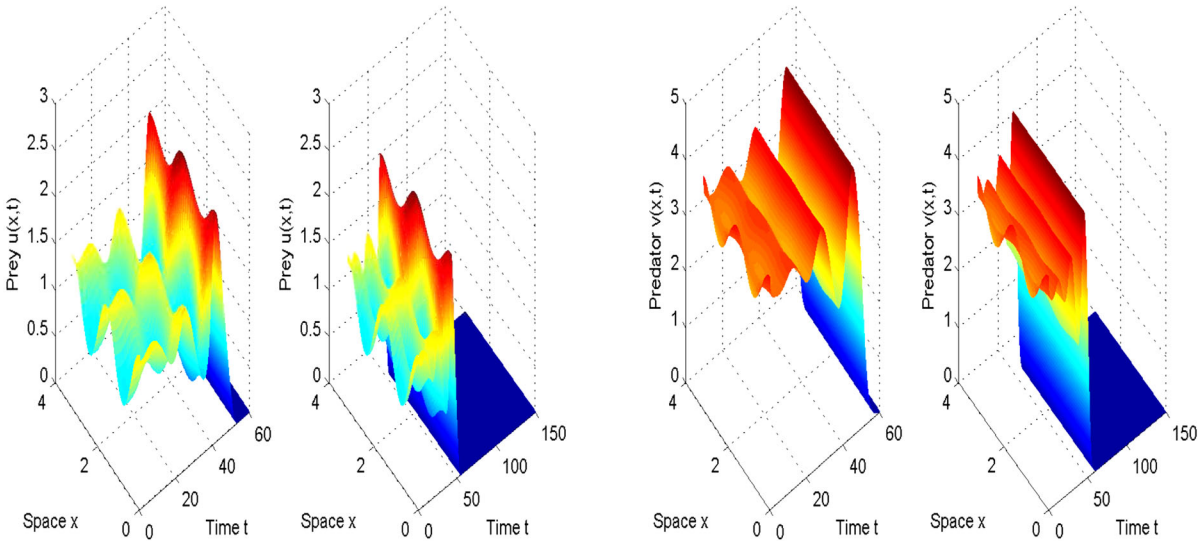


**Fig. 12** Numerical simulation of system (1.4) for $d_1 = 0.02, d_2 = 0.2, a = 2.5, b = 4.5, c = 0.6$. The positive equilibrium $E^*(1.26, 3.78)$ is unstable, and an unstable steady state solution like $\cos 4x$ shape emerges. Finally, the system evolves into the zero solution. The initial values are $u(x, 0) = 1.26 + 0.4\cos 4x$, $v(x, 0) = 3.78 + 0.4\cos 4x$

### 4.2 Hopf bifurcations and spatially homogeneous and inhomogeneous periodic solutions

When $a > 1.6089$, the first bifurcation when $b$ increases is a Hopf bifurcation. To demonstrate this numerically, we take $a = 2.5$. Figure 9 illustrates the bifurcation diagram in the $b-k$ plane. There exist Hopf bifurcations on $H_0$ and $H_1$ as well as eight steady state bifurcation points $O_k, k = 1, 2, \ldots, 8$. As $b$ increases, system (1.4) first undergoes Hopf bifurcation on $H_0$ and then steady state bifurcation at $O_3$, Hopf bifurcation on $H_1$, and so on. The positive equilibrium $E^*$ is

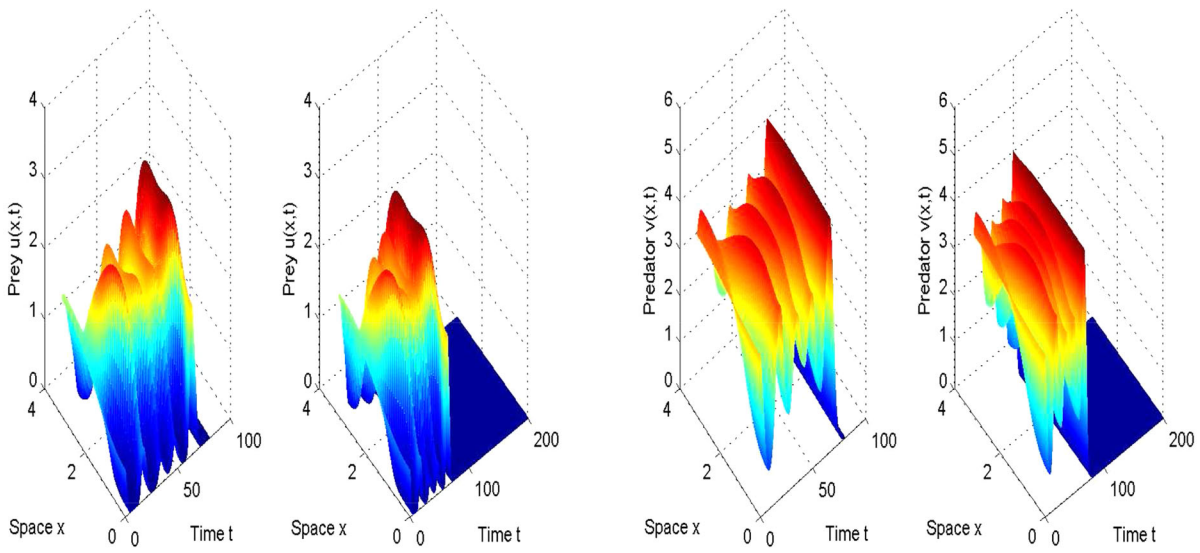


**Fig. 13** Numerical simulation of system (1.4) for $d_1 = 0.02, d_2 = 0.2, a = 2.5, b = 4.7, c = 0.6$. The positive equilibrium $E^*(1.1656, 3.6522)$ is unstable, and the system finally evolves into the zero solution. The initial values are $u(x, 0) = 1.1656 - 0.5\cos x$, $v(x, 0) = 3.6522 - 0.2\cos x$

asymptotically stable for $0 < b < 4.2813$ and unstable for $b > 4.2813$. For the Hopf bifurcation on $H_0$, by (3.39) and using the software Matlab, we can obtain the following normal form truncated to the third-order term:

$$\dot{\rho} = 0.3200\mu\rho - 0.0127\rho^3.$$

So, the Hopf bifurcation on $H_0$ is supercritical and stable. Taking $b = 4.3$ as example which is larger than the first Hopf bifurcation value $b = 4.2813$ and less than Turing bifurcation value $b = 4.3803$, a *spatially homogenous* stable periodic orbit bifurcates from the positive equilibrium $E^*$, as is shown in Fig. 10. When $b$ increases to pass the value 4.3803 (see $O_3$ in Fig. 10), a steady state bifurcation occurs. Since the characteristic equation (2.6) has at least a pair of roots with positive real parts for $b > 4.2813$, these steady state bifurcations must be unstable in the full phase space. Figures 11 and 12 illustrate the dynamics of system (1.4) for $b = 4.39$ close to $O_3$ and $b = 4.5$ close to $O_4$, respectively. Figures 11 and 12 show the existence of unstable nonconstant steady state with $\cos 3x$-like and $\cos 4x$-like shapes, respectively. Due to the interaction between Hopf and steady state bifurcations, the oscillatory dynamics in time only stay for a short period of time. At $b = 4.625$, system (1.4) undergoes Hopf bifurcation on $H_1$. This Hopf bifurcation leads to *spatially inhomogeneous* periodic solution with $\cos x$-like shape in space, which is unstable since the existence of positive real roots and roots with positive real parts. Figure 13 illustrates the dynamics of the system at $b = 4.7$.

## 5 Conclusion

In this paper, we have studied a ratio-dependent predator–prey model with diffusion. We have obtained sufficient and necessary conditions for the stability and Turing instability of the positive constant equilibrium. We have also rigorously proved that if the diffusion coefficient of prey is greater ($d_1 \geq d_2 c(1-c)/[d_2 + c(1-c)] > 0$), there is no diffusion-driven instability, and if it is smaller ($0 < d_1 < d_2 c(1-c)/[d_2 + c(1-c)]$), a diffusion-driven instability will occur at some critical values. For fixed normalized death rate $c$ of predator, we have identified the boundaries of the regions in the parameter $b - a$ plane for the stability and Turing instability, as well as curves for Hopf and steady state bifurcations. The spatial structure associated with Turing instability can also be explicitly determined. The $a-$axis can be divided into a sequence of intervals. Each interval corresponds to certain spatial structure.

With the help of normal forms on the center manifold, the formulas determining the direction and sta-

bility of Hopf bifurcations and the patterns of steady state bifurcations are derived. The calculation of normal forms for the steady state bifurcation shows that there exists a pitchfork bifurcation with two spatially inhomogeneous steady states. Numerical simulations illustrate the spatially stable homogeneous and unstable inhomogeneous periodic solutions and the coexistence of two spatially inhomogeneous steady states through the pitchfork bifurcation.

**Acknowledgments** The first author is supported by the State Key Program of National Natural Science of China (No. 11032009), the Scientific Research Foundation for the Returned Overseas Chinese Scholars, the Fundamental Research Funds for the Central Universities, and the Program for New Century Excellent Talents in University (NCET-11-0385); and the second author is partially supported by Natural Science and Engineering Council of Canada.

## References

1. Akcakaya, H.R., Arditi, R., Ginzburg, L.R.: Ratio-dependent prediction: an abstraction that works. Ecology **76**, 995–1004 (1995)
2. Aly, S., Kim, I., Sheen, D.: Turing instability for a ratio-dependent predator–prey model with diffusion. Appl. Math. Comput. **217**, 7265–7281 (2011)
3. Allesina, S., Tang, S.: Stability criteria for complex ecosystems. Nature **483**, 205–208 (2012)
4. Arditi, R., Berryman, A.A.: The biological control paradox. Trends Ecol. Evol. **6**, 32 (1991)
5. Arditi, R., Ginzburg, L.R.: Coupling in predator–prey dynamics: ratio-dependence. J. Theor. Biol. **139**, 311–326 (1989)
6. Arditi, R., Ginzburg, L.R., Akcakaya, H.R.: Variation in plankton densities among lakes: a case for ratio-dependent models. Am. Nat. **138**, 1287–1296 (1991)
7. Arino, O., El abdllaoui, A., Mikram, J., Chattopadhyay, J.: Infection in prey population may act as a biological control in ratio-dependent predator–prey models. Nonlinearity **17**, 1101–1116 (2004)
8. Aronson, D.G., Weinberger, H.F.: Nonlinear diffusion in population genetics, combustion, and nerve pulse propagation. In: Partial Differential Equations and Related Topics, Lecture Notes in Math., Vol. 446, Springer, Berlin (1975)
9. Astrom, M.: The paradox of biological control revisited: per capita non-linearities. Oikos **78**, 618–621 (1997)
10. Banerjee, M.: Self-replication of spatial patterns in a ratio-dependent predator–prey model. Math. Comput. Model. **51**, 44–52 (2010)
11. Banerjee, M., Petrovskii, S.: Self-organised spatial patterns and chaos in a ratio-dependent predator–prey system. Theor. Ecol. **4**, 37–53 (2011)
12. Bartumeus, F., Alonsoa, D., Catalana, J.: Self-organized spatial structures in a ratio-dependent predator–prey model. Physica A **295**, 53–57 (2001)
13. Beretta, E., Kuang, Y.: Global analyses in some delayed ratio-dependent predator–prey systems. Nonlinear Anal., T.M.A. **32**, 381–408 (1998)
14. Berryman, A.A.: The origin and evolution of predator–prey theory. Ecology **73**, 1530–1535 (1992)
15. Carr, J.: Applications of Center Manifold Theory. Springer, New York (1981)
16. Chow, S.N., Hale, J.K.: Methods of Bifurcation Theory. Springer, New York (1982)
17. Cosner, C., DeAngelis, D.L., Ault, J.S., Olson, D.B.: Effects of spatial grouping on the functional response of predators. Theor. Pop. Biol. **56**, 65–75 (1999)
18. Deng, B., Jessie, S., Ledder, G., Rand, A., Strodulski, S.: Biological control does not imply paradox. Math. Biosci. **208**, 26–32 (2007)
19. Fan, Y.H., Li, W.T.: Global asymptotic stability of a ratio-dependent predator–prey system with diffusion. J. Comput. Appl. Math. **188**, 205–227 (2006)
20. Fan, M., Wang, Q., Zou, X.: Dynamics of a non-autonomous ratio-dependent predator–prey system. Proc. R. Soc. Edinb. A **133**, 97–118 (2003)
21. Faria, T.: Normal forms and Hopf bifurcation for partial differential equations with delay. Trans. Am. Math. Soc. **352**, 2217–2238 (2000)
22. Gause, G.F.: The Struggle for Existence. Williams and Wilkins, Baltimore (1935)
23. Hairston, N.G., Smith, F.E., Slobodkin, L.B.: Community structure, population control and and competition. Am. Nat. **94**, 421–425 (1960)
24. Hsu, S.-B., Hwang, T.-W., Kuang, Y.: Global analysis of the Michaelis–Menten type ratio-dependent predator–prey system. J. Math. Biol. **42**, 489–506 (2001)
25. Hsu, S.-B., Hwang, T.-W., Kuang, Y.: Rich dynamics of a ratio-dependent one prey two predator model. J. Math. Biol. **43**, 377–396 (2001)
26. Jost, C., Arino, O., Arditi, R.: About deterministic extinction in ratio-dependent predator–prey models. Bull. Math. Biol. **61**, 19–32 (1999)
27. Kuang, Y., Beretta, E.: Global qualitative analysis of a ratio-dependent predator–prey system. J. Math. Biol. **36**, 389–406 (1998)
28. Kuang, Y.: Rich dynamics of Gause-type ratio-dependent predator–prey systems. Fields Inst. Commun. **21**, 325–337 (1999)
29. Kuznetsov, Y.A.: Elements of Applied Bifurcation Theory, 2nd edn. Springer, New York (1998)
30. Luck, R.F.: Evaluation of natural enemies for biological control: a behavioral evaluation. Trends Ecol. Evol. **5**, 196–199 (1990)
31. Murray, J.D.: Mathematical Biology II. Springer, Heidelberg (2002)
32. Okubo, A., Levin, S.: Diffusion and Ecological Problems: Modern Perspectives. Springer, Berlin (2001)
33. Pang, P.Y.H., Wang, M.: Qualitative analysis of a ratio-dependent predator–prey system with diffusion. Proc. R. Soc. Edinb. A **133**, 919–942 (2003)

34. Peng, R., Shi, J.: Non-existence of non-constant positive steady states of two Holling type-II predator–prey systems: strong interaction case. J. Differ. Equ. **247**, 866–886 (2009)
35. Rosenzweig, M.L.: Paradox of enrichment: destabilization of exploitation systems in ecological time. Science **171**, 385–387 (1971)
36. Ruan, S., Tang, Y., Zhang, W.: Versal unfoldings of predator–prey systems with ratio-dependent functional response. J. Differ. Equ. **249**, 1410–1435 (2010)
37. Song, Y., Zou, X.: Spatiotemporal dynamics in a diffusive ratio-dependent predator-prey model near a Hopf-Turing bifurcation point. Comput. Math. Appl. doi:10.1016/j.camwa.2014.04.015
38. Turing, A.M.: The chemical basis of morphogenesis. Philos. Trans. R. Soc. Lond. B. **237**, 37–72 (1952)
39. Wang, J., Shi, J., Wei, J.: Dyanmics and pattern formation in a diffusive predator–prey system with strong Allee effect in prey. J. Differ. Equ. **251**, 1276–1304 (2011)
40. Wang, W., Liu, Q.X., Jin, Z.: Spatiotemporal complexity of a ratio-dependent predator–prey system. Phys. Rev. E **75**, 051913–051921 (2007)
41. Wiggins, S.: Introduction to Applied Nonlinear Dynamical Systems and Chaos. Springer, New York (2003)
42. Wu, J.: Theory and Applications of Partial Functional Differential Equations. Springer, New York (1996)
43. Xiao, D., Ruan, S.: Global dynamics of a ratio-dependent predator–prey systems. J. Math. Biol. **43**, 221–290 (2001)
44. Xiao, D., Li, W.: Stability and bifurcation in a delayed ratio-dependent predator–prey system. Proc. Edinb. Math. Soc. **45**, 205–220 (2003)
45. Xu, R., Davidson, F.A., Chaplain, M.A.J.: Persistence and stability for a two-species ratio-dependent predator–prey system with distributed time delay. J. Math. Anal. Appl. **269**, 256–277 (2002)
46. Yi, F., Wei, J., Shi, J.: Bifurcation and spatiotemporal patterns in a homogeneous diffusive predator–prey system. J. Differ. Equ. **246**, 1944–1977 (2009)
47. Zhang, J., Li, W., Yan, X.: Hopf bifurcation and turing instability in spatial homogeneous and inhomogeneous predator–prey models. Appl. Math. Comput. **218**, 1883–1893 (2011)